

# Centrality and topology properties in a tree-structured Markov random field

Benjamin Côté, Hélène Cossette, Etienne Marceau

*École d'actuariat, Université Laval, Québec, Canada*

October 26, 2024

## Abstract

The topology of the tree underlying a tree-structured Markov random field (MRF) is central to the understanding of its stochastic dynamics: it is, after all, what synthesizes the rich dependence relations within the MRF. In this paper, we shed light on the influence of the tree's topology, through an extensive comparison-based analysis, on the aggregate distribution of the MRF. This is done within the framework of a recently introduced family of tree-structured MRFs with the uncommon property of having fixed Poisson marginal distributions unaffected by the dependence scheme. We establish convex orderings of sums of MRFs encrypted on trees having different topologies, leading to the devising of a new poset of trees. Hasse diagrams, cataloguing trees of dimension up to 9, and methods for the comparison of higher-dimension trees are provided to offer an exhaustive investigation of the new poset. We also briefly discuss its relation to other existing posets of trees and to invariants from spectral graph theory. Such an analysis requires, beforehand, to study the joint distribution of a MRF's component and its sum, a random vector we refer to as a *synecdochic pair*. To assess if a component is less or more contributing than another to the sum, we employ stochastic orders to compare synecdochic pairs within a MRF. The resulting orderings are reflected through allocation-related quantities, which thus act as centrality indices.

**Keywords:** multivariate Poisson distributions, undirected graphical models, dependence trees, supermodular order, convex order, tree-shape partial order, network centrality.

## 1 Introduction

High-dimensional count data often exhibit complex dependence relations, motivating the need for efficient models to capture them through an intelligible representation. Markov random fields (MRF), also called *Markov networks* or *undirected graphical models*, are convenient for this matter as their underlying graph offers an at-glance understanding of the conditional independencies at play. The graph thus becomes an intuitive visual schematization of the stochastic dynamics underlying the MRF. We focus on trees, a family of graphs convenient given their cycle-free nature. As highlighted in [Gölpek, 2024], trees have prominent value in computer science and data analytics and are most often the means to break down problems involving general graphs. Moreover, in the context of MRFs, tree structures allow for exact belief propagation algorithms and hence offer a method of approximation for general graph-based MRFs (see [Wainwright et al., 2003]).

The literature on probabilistic graphical models has seen much emphasis been put on the recovery of the underlying tree from high dimensional data ([Bresler and Karzand, 2020], [Chow and Liu, 1968], [Hue and Chiogna, 2021], [Nikolakis et al., 2021]). To fully exploit the intelligibility of MRFs, it is crucial to develop tools for the interpretation of this resulting tree and its effect on the joint distribution of the MRF. This is the aim of this paper. In this vein, we rely on stochastic orders for a comparison-based understanding of the effect of the underlying tree's topology (shape) on MRFs' distributions. Our discussion takes two angles, by addressing the following questions:

Which of two vertex positions grants more influence on the overall dynamics? (Q1)

Which of two shapes of trees yields a riskier aggregate distribution? (Q2)

To properly answer (Q1) and (Q2), one needs to single out the effect of an alteration in the shape of the tree. This matter is not trivial for most families of MRFs, since modifying the shape of their underlying tree would also alter their marginal distributions and thus befog its effect on the dependence. In [Côté et al., 2024], the authors introduced a new family of tree-structured MRFs, whose collection of distributions we denote by  $\text{MMPMRF}$ . A specific property of these MRFs is their fixed marginal Poisson distributions: every component of the MRF follows a Poisson distribution of identical mean. Here, *fixed* refers to the fact that changing the value of dependence parameters or the underlying tree of the joint distribution of the MRFs does not affect the marginal distributions; this property is uncommon for MRFs. The family  $\text{MMPMRF}$  will be the vehicle of our discussions, leveraging on this key feature, to uncover, *ceteris paribus*, the true effect of the underlying shape on the joint distributions of the MRFs. One should see this work as a stepping stone to extending the discussion to more classes of MRFs. The family  $\text{MMPMRF}$  must not be confused with the auto-Poisson distributions presented in [Besag, 1974], and commonly referred to as *Poisson graphical models* such as in the review on multivariate Poisson distributions in [Inouye et al., 2017]. The family of distributions examined in [Kızıldemir and Privault, 2017] must not either be mistaken with  $\text{MMPMRF}$ .

We examine the joint distribution of a given component of a MRF and the sum of all its components to address (Q1). We use the term *synecdochic* as a qualifier to refer to this specific pair of random variables, as we recall a synecdoche establishes a semantic link between a part and its whole. We compare synecdochic pairs using stochastic orders to establish which components of the MRF are more contributing to the sum than others, to answer (Q1). These comparisons will invite the notion of a vertex’s centrality in a network, a concept notably studied in social sciences (see [Borgatti et al., 2009, Schoch, 2015] for contextualization; seminal works include [Borgatti, 2005], [Borgatti et al., 2024], [Freeman, 1979] and [Friedkin, 1991]). Our analysis contributes to transfer frameworks and manners of thought specific to network centrality theory to the legibility of probabilistic graphical models. We furthermore connect this analysis to quantities involved in risk allocation problems.

In regard to (Q2), we consider MRFs defined on trees of different topologies and investigate how their aggregate distributions’ riskiness may be compared using the convex order. Remark 1 of [Côté et al., 2024] states that no supermodular order may be established between members of  $\text{MMPMRF}$  when underlying trees have different shapes. However, thanks to synecdochic pairs’ ordering results derived for (Q1), it is still possible to establish convex orderings for distributions of sums. This allows new perspectives in the study of MRFs, which we explore for  $\text{MMPMRF}$  through the design of a new tree-comparing partial order. We then derive multiple results with the goal of facilitating comparisons with this new partial order; notably, we trace Hasse diagrams offering an exhaustive look at relations between trees of  $d = \{4, 5, 6, 7, 8, 9\}$  vertices, and provide means of comparing trees of higher dimensions. We also discuss the new partial order’s connections to other existing posets, and, in that vein, its relation to spectral graph theory.

We recall some results on  $\text{MMPMRF}$ , in Section 2, before addressing (Q1) in Section 3 and (Q2) in Section 4. In Section 4, we also discuss how (Q1) and (Q2) are connected to each other.

## 2 Tree-structured MRFs with Poisson marginal distributions

In this section, we provide a summary of key results derived in [Côté et al., 2024] pertaining to the family of distributions  $\text{MMPMRF}$ . We begin with some definitions and notation.

Consider a set of vertices  $\mathcal{V} = \{1, 2, \dots, d\}$ ,  $d \in \mathbb{N}_1 = \mathbb{N} \setminus \{0\}$ , and a set of edges  $\mathcal{E} \subseteq \mathcal{V} \times \mathcal{V}$ . In this paper, no loops are allowed, meaning that, for  $u \in \mathcal{V}$ ,  $(u, u) \notin \mathcal{E}$ , and the edges are undirected, meaning that, for  $u, v \in \mathcal{V}$ , if  $(u, v) \in \mathcal{E}$ , then  $(v, u)$  is the same element of  $\mathcal{E}$ . A simple, undirected graph  $\mathcal{G}$  is given by the coalescence of  $\mathcal{V}$  and  $\mathcal{E}$ , written  $\mathcal{G} = (\mathcal{V}, \mathcal{E})$ . For a graph  $\mathcal{G}$ , a path from a vertex  $u$  to a vertex  $v$ , denoted by  $\text{path}(u, v)$ , is a set of edges such that  $u$  and  $v$  participates in only one edge, while every other involved vertex participates in an even number of edges. We say these vertices are *on* the path. A tree, denoted by  $\mathcal{T}$ , is a graph where one and only one path exists for any pair of vertices. A tree thus has  $d - 1$  edges. For a tree  $\mathcal{T}$ , one may choose a vertex  $r \in \mathcal{V}$  to be the *root*. The rooted version of the tree is then denoted by  $\mathcal{T}_r$ . Choosing a root allows to refer to vertices on a tree according to their relative positions to one another, as the following filial relations become well defined. For a rooted tree  $\mathcal{T}_r$ , the descendants of vertex  $v \in \mathcal{V}$ , denoted by  $\text{dsc}(v)$ , is the set of vertices for which  $v$  is on their

path to the root,  $\text{dsc}(v) = \{u \in \mathcal{V} : \exists w \in \mathcal{V}, (v, w) \in \text{path}(u, r)\}$ ,  $v \in \mathcal{V}$ . The children of  $v$ , denoted by  $\text{ch}(v)$ , is the set of its descendants also participating in an edge with it,  $\text{ch}(v) = \{j \in \text{dsc}(v) : (v, j) \in \mathcal{E}\}$ ,  $v \in \mathcal{V}$ . The parent of  $v$ , denoted by  $\text{pa}(v)$ , is the sole vertex participating with it in an edge that is not its children; it is incidentally the first vertex on its path to the root. The root  $r$  has no parent. We recommend Chapter 3 of [Saoub, 2021] for an introduction to rooted trees and filial relations between vertices.

Following the definition in Section 4.2 of [Cressie and Wikle, 2015], a vector of random variables  $\mathbf{X} = (X_v, v \in \mathcal{V})$  is a MRF defined on a tree  $\mathcal{T} = (\mathcal{V}, \mathcal{E})$  if it satisfies the local Markov property, that is, for any two of its components, say  $X_u$  and  $X_w$ , such that  $(u, w) \notin \mathcal{E}$ ,

$$X_u \perp\!\!\!\perp X_w \left| \left\{ X_j, (u, j) \in \mathcal{E} \right\}, \quad (1)$$

where  $\perp\!\!\!\perp$  denotes conditional independence. Given Lemma 1 of [Matúš, 1992], the local Markov property is equivalent to the global Markov property on a tree. A tree-structured MRF therefore satisfies

$$X_u \perp\!\!\!\perp X_w \left| \left\{ X_j, j \in S(u, w) \right\}, \quad u, w \in \mathcal{V}, \quad (2)$$

where  $S(u, w)$  is a separator for  $u$  and  $w$ , a set of vertices such that every path from  $u$  to  $w$  has at least one participating vertex from that set. On a tree,  $S(u, w)$  is any vertex on  $\text{path}(u, w)$ . Chapter 3 of [Lauritzen, 1996] provides a discussion on the Markov properties for probabilistic graphical models.

Characterizing the family of distributions  $\text{MPMRF}$  is a stochastic representation relying on the binomial thinning operator, denoted by  $\circ$ , introduced in [Steutel et al., 1983]. For a count random variable  $N$  and a thinning parameter  $\alpha \in (0, 1)$ , binomial thinning is the operation  $\alpha \circ N = \sum_{i=1}^N I_i^{(\alpha)}$ , where  $\{I_i^{(\alpha)}, i \in \mathbb{N}_1\}$  is a sequence of independent Bernoulli random variables taking 1 with probability  $\alpha$ , and with the convention  $\sum_{i=1}^0 x_i = 0$ . We hereby transcribe Theorem 1 of [Côté et al., 2024] providing the stochastic representation.

**Theorem 1** (Stochastic representation). *Given a tree  $\mathcal{T} = (\mathcal{V}, \mathcal{E})$  and a chosen root  $r \in \mathcal{V}$ , let  $\mathcal{T}_r$  be its rooted version. Consider a vector of dependence parameters  $\alpha = (\alpha_e, e \in \mathcal{E})$ ,  $\alpha \in (0, 1)^{d-1}$  and define  $\mathbf{L} = (L_v, v \in \mathcal{V})$  as a vector of independent random variables such that  $L_v \sim \text{Poisson}(\lambda(1 - \alpha_{(\text{pa}(v), v)}))$ ,  $\lambda > 0$ , for  $v \in \mathcal{V}$ , with the convention  $\alpha_{(\text{pa}(r), r)} = 0$  since the root has no parent. Let  $\mathbf{N} = (N_v, v \in \mathcal{V})$  be a vector of count random variables whose components are defined by*

$$N_v = \begin{cases} L_r, & v = r \\ L_v + \alpha_{(\text{pa}(v), v)} \circ N_{\text{pa}(v)}, & v \in \text{dsc}(r) \end{cases}, \quad \text{for every } v \in \mathcal{V}. \quad (3)$$

Then,  $\mathbf{N}$  is a tree-structured MRF with Poisson marginal distributions of parameter  $\lambda$ . Throughout the paper, we take the convention of writing  $\mathbf{N} \sim \text{MPMRF}(\lambda, \alpha, \mathcal{T})$ .

The stochastic construction in (3) always leads to a valid multivariate Poisson distribution. Moreover, as stated in Theorem 2 of [Côté et al., 2024], the choice of the root  $r \in \mathcal{V}$  in (3) has no impact on the joint distribution of  $\mathbf{N}$ . Choosing a root simply offers convenience for notation, proofs and programming purposes. We hereby transcribe the expression of the joint probability generating function (pgf) of  $\mathbf{N}$ , which will be useful throughout the paper. For notation purposes, let  $\text{vdsc}(v) = \{v\} \cup \text{dsc}(v) \subseteq \mathcal{V}$  and let  $\mathbf{t}_{\text{vdsc}(v)} = (t_j, j \in \text{vdsc}(v))$ , for  $v \in \mathcal{V}$ . Assuming that  $\mathbf{N} \sim \text{MPMRF}(\lambda, \alpha, \mathcal{T})$  with  $\mathcal{T} = (\mathcal{V}, \mathcal{E})$ , and, for a chosen root  $r \in \mathcal{V}$ , letting  $\mathcal{T}_r$  be the rooted version of  $\mathcal{T}$ , the joint pgf of  $\mathbf{N}$  is given by

$$\mathcal{P}_{\mathbf{N}}(\mathbf{t}) = \mathbb{E} \left[ \prod_{v \in \mathcal{V}} t_v^{N_v} \right] = \prod_{v \in \mathcal{V}} e^{\lambda(1 - \alpha_{(\text{pa}(v), v)}) (\eta_v^{\mathcal{T}_r}(\mathbf{t}_{\text{vdsc}(v)}) - 1)}, \quad \mathbf{t} = (t_v, v \in \mathcal{V}) \in [-1, 1]^d, \quad (4)$$

where  $\eta_v^{\mathcal{T}_r}$ , for every  $v \in \mathcal{V}$ , is a joint pgf recursively defined as such:

$$\eta_v^{\mathcal{T}_r}(\mathbf{t}_{\text{vdsc}(v)}) = t_v \prod_{j \in \text{ch}(v)} \left( 1 - \alpha_{(v, j)} + \alpha_{(v, j)} \eta_j^{\mathcal{T}_r}(\mathbf{t}_{\text{jdsc}(j)}) \right), \quad (5)$$

with  $\eta_v^{\mathcal{T}_r}(\mathbf{t}_{\text{vdsc}(v)}) = t_v$  when  $\text{ch}(v) = \emptyset$ . The filial relations dictating the recursiveness of  $\eta_v^{\mathcal{T}_r}$  are taken according to the rooted tree in superscript.

Throughout, define the random variables  $M$  as the sum of the components of  $N$ , that is,  $M = \sum_{v \in \mathcal{V}} N_v$ . Consider  $N \sim \text{MPMRF}(\lambda, \alpha, \mathcal{T})$  with  $\mathcal{T} = (\mathcal{V}, \mathcal{E})$  and  $N' \sim \text{MPMRF}(\lambda, \alpha', \mathcal{T}')$  with  $\mathcal{T}' = (\mathcal{V}', \mathcal{E}')$ , with identical dependence parameter for every edge, meaning  $\alpha_e = \alpha$  for every  $e \in \mathcal{E}$  and  $\alpha'_e = \alpha$  for every  $e \in \mathcal{E}'$ ,  $\alpha \in (0, 1)$ . Suppose  $\mathcal{E} \neq \mathcal{E}'$ . Hence, the only difference in the respective distributions of  $N$  and  $N'$  comes from the distinct topologies (shapes) of trees  $\mathcal{T}$  and  $\mathcal{T}'$ . We are interested in the distributions of  $M$  and  $M'$ . In Section 7 of [Côté et al., 2024], the authors observe through numerical examples that the underlying tree itself seems to have an impact on the distribution of the sum of the MRFs. The next challenge is to find a criterion related to the shapes of the trees  $\mathcal{T}$  and  $\mathcal{T}'$  allowing to compare  $M$  and  $M'$  within the rigorous framework provided by the theory of stochastic orders. Before doing so, we need to investigate the contribution of the component  $N_v$  and the contribution of the component  $N_w$  on the distribution of  $M$  with regards to their positions within the tree  $\mathcal{T}$ ; this is done in the next section.

### 3 Comparison of synecdochic pairs

To answer the question (Q1), we examine the joint distribution of a component of the random vector  $N$  and its sum, that is, for a given vertex  $v \in \mathcal{V}$ , the joint distribution of the synecdochic pair  $(N_v, M)$ . Let us preface this section with an example, which requires the following definition to motivate this examination.

**Definition 1** (Supermodular Order). *Two vectors of random variables,  $X$  and  $X'$ , are ordered according to the supermodular order, denoted by  $X \leq_{sm} X'$ , if  $E[\zeta(X)] \leq E[\zeta(X')]$  for every supermodular function  $\zeta$ , given the expectations exist. A supermodular function  $\zeta : \mathbb{R}^d \mapsto \mathbb{R}$  is such that  $\zeta(\mathbf{x}) + \zeta(\mathbf{x}') \leq \zeta(\mathbf{x} \wedge \mathbf{x}') + \zeta(\mathbf{x} \vee \mathbf{x}')$ , holds for all  $\mathbf{x}, \mathbf{x}' \in \mathbb{R}^d$ , with  $\wedge$  denoting the componentwise minimum and  $\vee$  the componentwise maximum.*

Recall that, in the bivariate case, Definition 2 amounts to  $(X_1, X_2) \leq_{sm} (X'_1, X'_2)$  if  $F_{X_1, X_2}(x_1, x_2) \leq F_{X'_1, X'_2}(x_1, x_2)$ , for all  $(x_1, x_2) \in \mathbb{R}^2$ , that is, the supermodular order corresponds to the concordance order. We prefer to employ  $\leq_{sm}$  as it will be necessary for upcoming proofs. We recommend Chapters 1 and 2 of [Müller and Stoyan, 2002] and Chapters 3 and 9 of [Shaked and Shanthikumar, 2007] for an introduction to these stochastic orders and their applications.

**Example 1.** *Assume  $\mathcal{T} = (\mathcal{V}, \mathcal{E})$  is the 10-vertex star tree depicted in Figure 1 and consider  $N \sim \text{MPMRF}(1, \alpha, \mathcal{T})$ , with  $\alpha = (0.5 \mathbf{1}_{|\mathcal{E}|})$ , where  $\mathbf{1}_k$  is a  $k$ -long vector of 1's, meaning every edge has the same parameter. The specific shape  $\mathcal{T}$  makes the value taken by  $N_1$  have a direct influence on the values of all other  $N_v$ ,  $v \in \mathcal{V}$ . This influence is reflected in the distribution of  $M$ . As a result, the covariance between  $M$  and  $N_1$  is greater than for other components: we have  $\text{Cov}(N_1, M) = 5.5$ , whereas  $\text{Cov}(N_i, M) = 3.5$ ,  $i = \{2, \dots, 10\}$ . Plotting the joint cdfs of  $(N_1, M)$  and  $(N_i, M)$ ,  $i = \{2, \dots, 10\}$ , we observe that the first curve dominates the others, see Figure 1. This suggests that the impact of a vertex's position goes beyond a simple ordering of covariances. Taking a more extensive perspective by examining the joint distribution of synecdochic pairs allows us to seize this impact more completely: the curves indeed indicate a supermodular ordering between  $(N_1, M)$  and  $(N_i, M)$ ,  $i \in \{2, \dots, 10\}$ . The objective is to provide a criterion based on the vertices' positions in  $\mathcal{T}$  for such an ordering.*

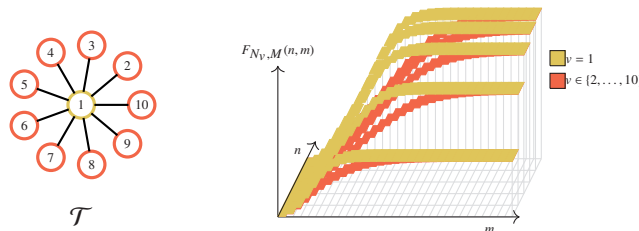


Figure 1: (Left) Tree  $\mathcal{T}$  from Example 1. (Right) Joint cdfs of the random vectors  $(N_v, M)$ ,  $v \in \mathcal{V} = \{1, \dots, 10\}$ .

The following definition describes the synecdochic pair's ordering observed in Example 1. It clarifies what is intended by *influence on the overall dynamics* in (Q1).

**Definition 2.** *Consider the vector of random variables  $X = (X_v, v \in \mathcal{V})$  and the sum of its components  $S = \sum_{v \in \mathcal{V}} X_v$ . For  $u, w \in \mathcal{V}$ , we say that  $X_u$  is less contributing than  $X_w$  to  $S$  if  $(X_u, S) \leq_{sm} (X_w, S)$ .*

Hence, in respect to Definition 2, we aim to compare the synecdochic pairs for distinct vertices  $v, w \in \mathcal{V}$  with regards to their positions within the tree  $\mathcal{T}$ . The key result of this section is given in Theorem 2, in which we provide the conditions to establish such comparisons through stochastic ordering. We then discuss how orderings of synecdochic pairs affect common quantities pertaining to risk allocation, and how this relates to the theory of network centrality.

As discussed in Section 3 of [Côté et al., 2024], the joint pgf of  $N$ , given in (4), highlights an alternative stochastic representation, which proves to be essential to the analysis of the joint distribution of synecdochic pairs. We formalize this result in Lemma 1 for easier referencing later on.

**Lemma 1.** *Given a tree  $\mathcal{T}$ , assume  $N = (N_v, v \in \mathcal{V}) \sim \text{MPMRF}(\lambda, \alpha, \mathcal{T})$  and, for a chosen root  $r \in \mathcal{V}$ , let  $\mathcal{T}_r$  be the rooted version of  $\mathcal{T}$ . For  $v \in \mathcal{V}$ , we define  $\mathbf{G}_v^{\mathcal{T}_r} = (G_{v,j}^{\mathcal{T}_r}, j \in \text{vdsc}(v))$  as a vector of discrete random variables whose joint pgf is  $\eta_v^{\mathcal{T}_r}$  as given by (5). Let  $H_v^{\mathcal{T}_r} = \sum_{j \in \text{vdsc}(v)} G_{v,j}^{\mathcal{T}_r}$ ; hence, its joint pgf is given by  $\eta_v^{\mathcal{T}_r}(t \mathbf{1}_{|\text{vdsc}(v)|})$ . Then,  $N$  and  $M$  admit the following alternative stochastic representations:*

$$N = \sum_{v \in \mathcal{V}} \sum_{k=1}^{L_v} \mathbf{G}_{v,(k)}^{\mathcal{T}_r}, \quad \text{and} \quad M = \sum_{v \in \mathcal{V}} \sum_{k=1}^{L_v} H_v^{\mathcal{T}_r}, \quad (6)$$

with sums taken componentwise according to the subscript  $j$ , and  $\{\mathbf{G}_{v,(k)}^{\mathcal{T}_r}, k \in \mathbb{N}_1\}$  being a sequence of independent vectors of random variables having the same joint distribution as  $\mathbf{G}_v^{\mathcal{T}_r}$ ,  $v \in \mathcal{V}$ , and independent of  $\mathbf{L}$  defined as in Theorem 1.

*Proof.* See equation (19) of [Côté et al., 2024] and comments therein.  $\square$

As for the sequences of joint pgfs  $\eta_v^{\mathcal{T}_r}$ ,  $r, v \in \mathcal{V}$  in (5), we specify in superscript the rooted tree on which  $\mathbf{G}_v^{\mathcal{T}_r}$  and  $H_v^{\mathcal{T}_r}$  define themselves, for the sake of clarity. A component  $G_{v,j}^{\mathcal{T}_r}$ ,  $j \in \text{vdsc}(v)$ , of  $\mathbf{G}_v^{\mathcal{T}_r}$ ,  $v, r \in \mathcal{T}_r$ , should be interpreted as such: it is the number of events having taken place at vertex  $v$  that have propagated to vertex  $j$  downward the tree  $\mathcal{T}$  according to a rooting in  $r$ . The stochastic representation of  $N$  in (6) then amounts to counting events after having classified them according to their origin in terms of propagation. Similarly, the random variable  $H_v^{\mathcal{T}_r}$  should be interpreted as the total number of events, occurring anywhere on the tree, originating from  $v$  according to a rooting in  $r$ . It thus summarizes the impact vertex  $v$  has on the other vertices down the tree, or if  $v = r$ , to all vertices in  $\mathcal{V}$ . Therefore, its distribution is the key to comparing synecdochic pairs. This elicits the criterion presented in the following theorem, characterizing, for the family MPMRF, the statement that a component contributes less than another to the sum  $M$ , as per Definition 2.

**Theorem 2.** *Given a tree  $\mathcal{T}$ , assume  $N = (N_v, v \in \mathcal{V}) \sim \text{MPMRF}(\lambda, \alpha, \mathcal{T})$  with  $\lambda > 0$  and  $\alpha \in (0, 1)^{d-1}$ , and let  $M = \sum_{v \in \mathcal{V}} N_v$ . We define the two discrete random variables  $H_v^{\mathcal{T}_v}$  and  $H_w^{\mathcal{T}_w}$  as in Lemma 1 with pgfs given by  $\mathcal{P}_{H_v^{\mathcal{T}_v}}(t) = \eta_v^{\mathcal{T}_v}(t \mathbf{1}_{|\text{vdsc}(v)|})$  and  $\mathcal{P}_{H_w^{\mathcal{T}_w}}(t) = \eta_w^{\mathcal{T}_w}(t \mathbf{1}_{|\text{vdsc}(w)|})$  as provided in (5),  $v, w \in \mathcal{V}$ ,  $t \in [-1, 1]$ . If*

$$H_v^{\mathcal{T}_v} \leq_{st} H_w^{\mathcal{T}_w}, \quad (7)$$

where  $\leq_{st}$  denotes the usual stochastic order, then  $(N_v, M) \leq_{sm} (N_w, M)$ , meaning that  $N_v$  is less contributing than  $N_w$  to  $M$  within the MRF  $N$ .

*Proof.* The proof is provided in Appendix A.  $\square$

Theorem 2 seems challenging to apply because one needs to verify the condition  $H_v^{\mathcal{T}_v} \leq_{st} H_w^{\mathcal{T}_w}$ . However, thanks to the recursive nature of the sequences of pgfs  $\{\eta_j^{\mathcal{T}_r}, j \in \mathcal{V}\}$ ,  $r \in \mathcal{V}$ , provided in (5), it is often not necessary to develop  $\mathcal{P}_{H_v^{\mathcal{T}_v}}(t)$  and  $\mathcal{P}_{H_w^{\mathcal{T}_w}}(t)$  completely to establish stochastic dominance. Other results pertaining to the criterion in (7) are explored later in Section 4, and examples showing first order stochastic dominance ordering between  $H_v^{\mathcal{T}_v}$  and  $H_w^{\mathcal{T}_w}$  are provided therein.

The condition  $H_v^{\mathcal{T}_v} \leq_{st} H_w^{\mathcal{T}_w}$  considers two different roots,  $v$  and  $w$ . Therefore, both random variables could not be part of the same stochastic representation given by (6). The choice of these roots is not anecdotal: for a root  $r \in \mathcal{V}$ , one has  $\text{rdsc}(r) = \mathcal{V}$ . The pgf given by  $\eta_v^{\mathcal{T}_v}(t \mathbf{1}_{|\text{vdsc}(v)|})$ , because of its recursive definition (5), thus encapsulates all the information needed on the shape of the tree, translating it into the distribution of  $H_v^{\mathcal{T}_v}$ ; likewise for  $H_w^{\mathcal{T}_w}$ ,  $v, w \in \mathcal{V}$ .

Theorem 2 states that, despite having identical marginal distributions, some random variables constituting the MRF  $N$  have more key roles in the distribution of  $M$  – are more contributing to  $M$ , as per Definition 2 – than others. As discussed in Chapter 9 of [Shaked and Shanthikumar, 2007], the supermodular order compares the strength of positive dependence within random vectors. The observations we have made in Example 1 are then confirmed by this result. The fact that the dependence within a synecdochic pair varies in strength depending on the vertices’ relative position in the tree relates to the notion of *centrality* of a vertex to the graph. Heuristically, the result of Theorem 2 suggests a vertex’s centrality should be understood as such in the stochastic context provided by the family MIPMRF: events occurring at the most central vertices are those which have the most possibilities to propagate to others, and reciprocally, these vertices also have the most chance of welcoming propagated events. This interpretation comes from that of  $H_v^T$ ,  $v \in \mathcal{V}$ , discussed above, arising from Lemma 1, and the criterion in (7). Accordingly, Theorem 2 indicates that if  $M$  has taken a high value, the random variables associated with these central vertices probably also had a high outcome since they are the most determinant to  $M$ . In [Freeman, 1979], the author explores the notion of centrality and highlights the fuzziness of what constitutes a vertex’s centrality. This is why we reason centrality following the dynamics at play on the graph, as advised and discussed in [Friedkin, 1991] and [Borgatti, 2005]. Centrality is generally understood regarding centrality indices; a discussion in the following subsection will confirm the coherence of our heuristic interpretation of the concept for the family MIPMRF.

The study of synecdochic pairs directly connects to risk allocation theory; one may consult [Overbeck, 2000], [Tasche, 2007] and [Dhaene et al., 2012] for an introduction on risk allocation concepts. We henceforth present a few relevant quantities. In Corollary 4 of [Côté et al., 2024], the authors discussed the expected allocation of  $N_v$  to  $M$  for a total outcome  $k \in \mathbb{N}$ , that is,  $E[N_v \mathbb{1}_{\{M=k\}}]$ ,  $v \in \mathcal{V}$  and gave its expression for the family MIPMRF. Expected allocations allow to perform risk management tasks such as risk-sharing and risk allocation, as they are notably employed in the computation of the conditional mean risk-sharing rule introduced in [Denuit and Dhaene, 2012], given by  $E[N_v | M = k] = E[N_v \mathbb{1}_{\{M=k\}}] / p_M(k)$ , with  $k \in \mathbb{N}$  such that  $p_M(k) > 0$ , and  $p_M$  denotes the pmf of  $M$ . A related quantity is the cumulative expected allocation, defined as  $E[N_v \mathbb{1}_{\{M \leq k\}}]$ , for  $k \in \mathbb{N}$ . Expected cumulative allocations are relevant to compute the contribution to the Tail-Value-at-Risk (TVaR) under Euler’s principle, as discussed in [Blier-Wong et al., 2022]. The risk measure TVaR at a confidence level  $\kappa$  is given by  $\text{TVaR}_\kappa(X) = \frac{1}{1-\kappa} \int_\kappa^1 \text{VaR}_u(X) du$ , with  $\text{VaR}_\kappa(X) = \inf\{x \in \mathbb{R} : F_X(x) \geq \kappa\}$ ,  $\kappa \in [0, 1)$ . Since  $M$  takes on values in  $\mathbb{N}$ , the contribution of  $N_v$ ,  $v \in \mathcal{V}$ , is given by

$$\begin{aligned} C_\kappa^{\text{TVaR}}(N_v; M) &= \frac{1}{1-\kappa} \left( E[N_v \mathbb{1}_{\{M > \text{VaR}_\kappa(M)\}}] + \frac{F_M(\text{VaR}_\kappa(M)) - \kappa}{p_M(\text{VaR}_\kappa(M))} E[N_v \mathbb{1}_{\{M = \text{VaR}_\kappa(M)\}}] \right) \\ &= \frac{1}{1-\kappa} \left( E[N_v] - E[N_v \mathbb{1}_{\{M \leq \text{VaR}_\kappa(M)\}}] + \frac{F_M(\text{VaR}_\kappa(M)) - \kappa}{p_M(\text{VaR}_\kappa(M))} E[N_v \mathbb{1}_{\{M = \text{VaR}_\kappa(M)\}}] \right), \end{aligned}$$

for  $\kappa \in [0, 1)$ ; see Section 2 in [Mausser and Romanko, 2018]. One easily verifies that  $\sum_{v \in \mathcal{V}} C_\kappa^{\text{TVaR}}(N_v; M) = \text{TVaR}_\kappa(M)$ . Contributions to TVaR represent the portion of the aggregate risk enclosed within each component of  $N$ . On a related note, the covariance  $\text{Cov}(N_v, M)$  pertains to the contribution of  $N_v$  to the standard deviation of  $M$  under Euler’s principle, and rather quantifies the portion of enclosed variability. One may consult [Tasche, 2007] for further insights on contributions to TVaR and to standard deviation under Euler’s rule.

The ordering of synecdochic pairs provided by Theorem 2 manifests itself through an ordering of covariances, expected cumulative allocations and contributions to TVaR under Euler’s rule, as a consequence of the following proposition.

**Proposition 1.** *If  $N_v$  is less contributing than  $N_w$  to  $M$ , with respect to Definition 2, then the following holds:*

- (a)  $\text{Cov}(N_v, M) \leq \text{Cov}(N_w, M)$ ;
- (b)  $E[N_v \mathbb{1}_{\{M \leq k\}}] \geq E[N_w \mathbb{1}_{\{M \leq k\}}]$ , for all  $k \in \mathbb{N}$ ;
- (c)  $C_\kappa^{\text{TVaR}}(N_v; M) \leq C_\kappa^{\text{TVaR}}(N_w; M)$ , for all  $\kappa \in [0, 1)$ .

*Proof.* The statements result from the supermodular ordering between  $(N_v, M)$  and  $(N_w, M)$  according to Definition 2. Theorem 3.8.2 of [Müller and Stoyan, 2002] grants the validity of part (a). It also states that the inequality  $E[N_v \mathbb{1}_{\{M \geq k\}}] \leq E[N_w \mathbb{1}_{\{M \geq k\}}]$  holds for every  $k \in \mathbb{N}$ , since  $x \mapsto \mathbb{1}_{\{x \geq k\}}$  is nondecreasing. Part (b) then ensues given  $E[N_v] = E[N_w]$ , and part (c) follows from Lemma 3 (see Appendix C).  $\square$

Based on the above discussion on centrality,  $\text{Cov}(N_v, M)$ ,  $E[N_v \mathbb{1}_{\{M \leq k\}}]$ , and  $C_k^{\text{TVaR}}(N_v, M)$  all act as centrality indices, as they induce an ordering of vertices within a tree, coherent with our understanding of centrality given Theorem 2. In the seminal paper [Freeman, 1979], the author, in a effort to dispel the reigning confusion around centrality, divided the notion into three concepts: degree, betweenness and closeness, and introduced the now-classical eponymous centrality indices. Freeman's closeness, in our tree-based context where only one path exists for each pair of vertices, is given by

$$c_v^{\text{clo}} = \sum_{j \in \mathcal{V}} |\text{path}(v, j)|, \quad v \in \mathcal{V}. \quad (8)$$

Having a *centrality* index increase when a vertex is farther in terms of path distances is counter-intuitive, as pointed out in [Borgatti and Everett, 2006]. Authors have suggested functional transformations for  $|\text{path}(v, j)|$  in (8) to remedy to this issue, such as the multiplicative inverse, yielding the harmonic closeness discussed in [Rochat, 2009], or an exponential transformation. The latter was proposed in [Burt, 1991], p. 66, and converts Freeman's closeness to

$$c_v^{\text{clo,exp.transf}} = \sum_{j \in \mathcal{V}} \alpha^{|\text{path}(v, j)|}, \quad v \in \mathcal{V}, \quad (9)$$

for a chosen parameter  $\alpha \in (0, 1)$ . In our context, the centrality index  $\text{Cov}(N_v, M)$ , from Proposition 1(a), is actually the index in (9), up to a multiplicative constant, with  $\alpha$  being the dependence parameter for the edges. Indeed, provided  $\text{Cov}(N_v, N_j) = \lambda \prod_{e \in \text{path}(v, j)} \alpha_e$  given Theorem 5 of [Côté et al., 2024], we have

$$\text{Cov}(N_v, M) = \sum_{j \in \mathcal{V}} \text{Cov}(N_v, N_j) = \lambda \sum_{j \in \mathcal{V}} \prod_{e \in \text{path}(v, j)} \alpha_e = \lambda \sum_{j \in \mathcal{V}} \alpha^{|\text{path}(v, j)|} = \lambda c_v^{\text{clo,exp.transf}},$$

where the fourth equality comes from the fact that  $\alpha_e = \alpha$  for every  $e \in \mathcal{E}$  under the assumptions of Theorem 2. The quantity  $\text{Cov}(N_v, M)$  is thus a closeness index in terms of Freeman's categorization.

Note that the ordering of vertices induced by index  $\text{Cov}(N_v, M)$  may not be the same as that of indices  $E[N_v \mathbb{1}_{M \leq k}]$ , as in Proposition 1(b), and  $C_k^{\text{TVaR}}(N_v, M)$ , as in Proposition 1(c), since the condition in (7) is sometimes not satisfied for two vertices  $v, w \in \mathcal{V}$ . Because of the intricacy of their respective analytical expressions, we cannot proceed as for  $\text{Cov}(N_v, M)$  and connect  $E[N_v \mathbb{1}_{M \leq k}]$  and  $C_k^{\text{TVaR}}(N_v; M)$  to other existing centrality indices. Nevertheless, the typology proposed in [Borgatti and Everett, 2006] suggests they be interpreted as closeness indices likewise. Indeed, as indicated by the expression given by Corollary 4 of [Côté et al., 2024], expected allocations indirectly takes into account the length of paths through the product of dependence parameters  $\alpha$  in  $\eta_v^{\mathcal{T}}(t \mathbf{1}_d)$ ,  $t \in [-1, 1]$ ,  $v \in \mathcal{V}$ . Moreover, the rooting in  $v$  suggests the paths considered by expected allocation all emanate from vertex  $v$  rather than flowing through it. We therefore deduce that the indices  $E[N_v \mathbb{1}_{\{M \leq k\}}]$  and  $C_k^{\text{TVaR}}(N_v; M)$  have a "length" Walk Property of and a "radial" Walk Position. Their cross-classification thus falls within the same category as Freeman's closeness and other closeness indices (see Table 1 of [Borgatti and Everett, 2006]).

One could want to verify if the three centrality indices put forth in Proposition 1 agree with axiomatic systems on centrality indices, such as [Sabidussi, 1966]'s and [Ruhnau, 2000]'s. However, these approaches were deemed reductive, as discussed earlier, by the authors of [Freeman, 1979], [Friedkin, 1991] and [Borgatti, 2005]: one needs to take into account the underlying dynamics occurring on the graph. There are no universal centrality index. As a matter of fact, axiomatic systems seem to consistently overlook closeness as a concept of centrality; one may refer to Table 3.2 in [Schoch, 2015] and the discussion thereabout. One should rather ask if the centrality indices are suitable to the context of the family MIPMRF. According to [Borgatti, 2005], the adequacy of a centrality index entails the flow of traffic – events, in our context – on the graph. The propagation dynamics unveiled by the stochastic representation in Theorem 1 gives an account of this flow of events. Events may propagate to multiple, but not necessarily all, neighbours at a time. Events follow paths, not walks, as they cannot propagate through the same edge back and forth. MIPMRF thus induces a *serial duplication, paths* flow of traffic. The conclusions of [Borgatti, 2005], summarized in Table 2 therein, suggest that closeness indices be preferred for contexts involving this type of flow on a tree. (Note that paths, geodesics and trails are the same on a tree.) Hence, from this reasoning, centrality indices from Proposition 1 would agree with the stochastic dynamics of MIPMRF.

## 4 Tree-shape partial order

Toward answering (Q2), forthcoming Theorem 3 exhibits how convex ordering may be established for  $M$ 's defined on underlying trees with different shapes. After, we devise a partial order induced by this result, allowing to compare trees on the basis of their shapes. Theorem 3 is therefore the cornerstone of this section.

**Definition 3** (Convex order). *Two random variables  $X$  and  $X'$  are said to be ordered according to the convex order, denoted by  $X \leq_{cx} X'$ , if  $E[\varphi(X)] \leq E[\varphi(X')]$  for every convex function  $\varphi$ , given the expectations exist.*

Let us also recall the notion of *subtree* of a tree. Precisely, a subtree  $\tau$  of a tree  $\mathcal{T} = (\mathcal{V}, \mathcal{E})$  is defined by the pair  $(\mathcal{V}^\tau, \mathcal{E}^\tau)$ , where  $\mathcal{V}^\tau$  is a subset of vertices,  $\mathcal{V}^\tau \subseteq \mathcal{V}$ , and  $\mathcal{E}^\tau$  is a subset of edges,  $\mathcal{E}^\tau \subseteq \mathcal{E}$ , such that  $\tau$  is a tree itself.

**Theorem 3.** *Consider two trees  $\mathcal{T} = (\mathcal{V}, \mathcal{E})$  and  $\mathcal{T}' = (\mathcal{V}, \mathcal{E}')$  such that  $\mathcal{E} \setminus \{(u, v)\} = \mathcal{E}' \setminus \{(u, w)\}$ , that is the only difference between  $\mathcal{T}$  and  $\mathcal{T}'$  is that  $u$  is connected to  $w$  in  $\mathcal{T}'$  rather than to  $v$  as in  $\mathcal{T}$ . Suppose  $N \sim \text{MPMRF}(\lambda, \alpha, \mathcal{T})$  and  $N' \sim \text{MPMRF}(\lambda, \alpha', \mathcal{T}')$ , with  $\lambda > 0$  and  $\alpha, \alpha' \in [0, 1]^{d-1}$  such that  $\alpha_e = \alpha'_e$  for every  $e \in \mathcal{E} \setminus \{(u, v)\}$  and  $\alpha_{(u,v)} = \alpha'_{(u,w)}$ . Let  $M$  and  $M'$  be sums of the respective components of  $N$  and  $N'$ . Consider the subtree  $\tau^\dagger = (\mathcal{V}^\dagger = \{u\} \cup \text{dsc}(u), \mathcal{E}^\dagger = \{(i, j) \in \mathcal{E} : i, j \in \mathcal{V}^\dagger\})$ , with descendants of  $u$  taken according to rooting  $\mathcal{T}_v$  or, equivalently,  $\mathcal{T}'_w$ . Pruning  $\mathcal{T}$  or  $\mathcal{T}'$  of  $\tau^\dagger$  yields the same residual subtree, which we denote  $\tau^*$ , that is,  $\tau^* = (\mathcal{V}^* = \mathcal{V} \setminus \mathcal{V}^\dagger, \mathcal{E}^* = \mathcal{E} \setminus (\{(u, v)\} \cup \mathcal{E}^\dagger) = \mathcal{E}' \setminus (\{(u, w)\} \cup \mathcal{E}^\dagger))$ . We define the two discrete random variables  $H_v^{\tau_v^\dagger}$  and  $H_w^{\tau_w^\dagger}$  as in Lemma 1 with pgfs given by  $\mathcal{P}_{H_v^{\tau_v^\dagger}}(t) = \eta_v^{\tau_v^\dagger}(t \mathbf{1}_{|\text{dsc}(v)|})$  and  $\mathcal{P}_{H_w^{\tau_w^\dagger}}(t) = \eta_w^{\tau_w^\dagger}(t \mathbf{1}_{|\text{dsc}(w)|})$  as provided in (5),  $v, w \in \mathcal{V}$ ,  $t \in [-1, 1]$ . If  $H_v^{\tau_v^\dagger} \leq_{st} H_w^{\tau_w^\dagger}$ , then  $M \leq_{cx} M'$ .*

*Proof.* The proof is provided in Appendix B. □

Figure 2 provides an example of two trees  $\mathcal{T}$  and  $\mathcal{T}'$  such that  $\mathcal{E} \setminus \{(u, v)\} = \mathcal{E}' \setminus \{(u, w)\}$ , as considered by Theorem 3. For each, we colored the subtree  $\tau^\dagger$  in yellow (light shade) and the subtree  $\tau^*$  in blue (dark shade).



Figure 2: Two trees differing only by the anchoring position of vertex  $u$

Let  $\leq_{sha}$  denote the tree-shape partial order on the set  $\Omega_{\mathcal{T}}$  of all trees defined such that  $\mathcal{T} \leq_{sha} \mathcal{T}'$  if  $M \leq_{cx} M'$  according to Theorem 3, where the respective distributions of  $M$  and  $M'$  are defined on  $\mathcal{T}$  and  $\mathcal{T}'$ , and have the same vector of dependence parameters  $\alpha$  such that  $\alpha_e = \alpha$ , for every  $e \in \mathcal{E} \cup \mathcal{E}'$ ,  $\alpha \in (0, 1)$ . Recall that a partial order consists of a homogeneous binary relation that is reflexive, antisymmetric and transitive. The relation  $\leq_{sha}$  directly inherits reflexivity and transitivity from  $\leq_{cx}$ ; for antisymmetry, one needs to suppose that no two tree shapes yield the same distribution of  $M$ . We conjecture this is the case, as even the cospectral, so-called *topological twin* trees presented in [McKay, 1977] render different distributions of  $M$ . Else, one could work with the quotient space given by the equivalence relation on trees yielding the same distribution of  $M$ , which we would also denote by  $\Omega_{\mathcal{T}}$  for convenience. Therefore, the order  $\leq_{sha}$  satisfying the three properties of partial orders on  $\Omega_{\mathcal{T}}$  makes  $(\Omega_{\mathcal{T}}, \leq_{sha})$  a partially ordered set (poset); one may consult Chapter 2 of [Nguyen et al., 2018] for an introduction to posets.

The poset  $(\Omega_{\mathcal{T}}, \leq_{sha})$  offers a framework to compare, based on the shape of their dependence structure, MRFs of the proposed family that are on the same basis regarding their magnitude and the strength of their dependence. Theorem 3 induces  $\leq_{sha}$ . Indeed, it is this result that enables the ordering of trees according to their shape. Leaning on the transitivity of partial orders, the following corollary exhibits that trees differing by more than one edge may be compared by iterative applications of Theorem 3.

**Corollary 1.** *Let  $\{\mathcal{T}^{<k>}, k \in \{1, \dots, d-2\}\} \subseteq \Omega_{\mathcal{T}}$  be a sequence of trees resulting from the iterative deconstruction of a star to a series tree, as depicted in Figure 3, and assume  $d \geq 4$ . Hence,  $\mathcal{T}^{<1>}$  is a  $d$ -vertex star tree and  $\mathcal{T}^{<d-2>}$  is a  $d$ -vertex series tree. We have the following ordering of trees:*

$$\mathcal{T}^{<d-2>} \leq_{sha} \mathcal{T}^{<d-3>} \leq_{sha} \dots \leq_{sha} \mathcal{T}^{<2>} \leq_{sha} \mathcal{T}^{<1>}.$$

*Proof.* We proceed in an iterative manner, meaning we establish the order relation at each step as we go from the star to the series tree, changing one edge at a time, as in Figure 3. Without loss of generality, we work with the vertices labelled as in Figure 3.

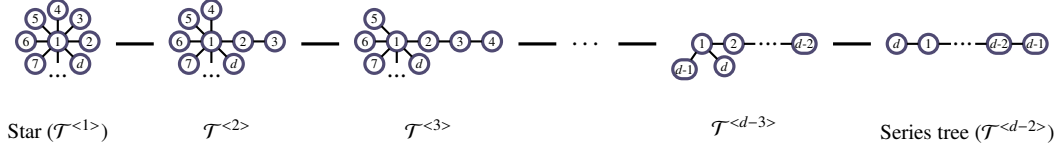


Figure 3: Iterative deconstruction of a star to a series tree.

We first look at  $\mathcal{T}^{<1>}$  and  $\mathcal{T}^{<2>}$ . They differ only from the anchorage of vertex 3, connected to 1 in the first case and to 2 in the second. In order to apply Theorem 3, we establish a stochastic dominance relation between  $H_1^{\tau^*}$  and  $H_2^{\tau^*}$ , defined on subtree  $\tau^*$  with vertices  $\mathcal{V}^* = \mathcal{V} \setminus \{3\}$ , in a context where all dependence parameters are equal to  $\alpha$ ,  $\alpha \in (0, 1)$ . Beforehand, we define  $\psi$  by

$$\psi(y, t, \alpha, \chi) = t(1 - \alpha + \alpha y)^\chi, \quad (10)$$

with  $\psi^{(k)}$  denoting the  $k$ th composition of  $\psi$  on  $y$ ,  $k \in \mathbb{N}_1$ , and  $\psi^{(0)}(y, t, \alpha, \chi) = t$ . Also, for Bernoulli random variables  $\{I_j, j \in \mathbb{N}_1\}$  and random variables  $X_1$  and  $X_2$ , note that  $X_1 + X_2 \times \prod_{j=1}^k I_j \leq_{st} X_1 + X_2$  for any  $k \in \mathbb{N}_1$ . Therefore, for random variables  $X_3$  and  $X_4$  with respective pgfs given by  $\mathcal{P}_{X_3}(t) = \psi^{(k)}(t\mathcal{P}_{X_2}(t), t, \alpha, 1)$  and  $\mathcal{P}_{X_4}(t) = \psi^{(k)}(t, t, \alpha, 1) \times \mathcal{P}_{X_2}(t)$ ,  $k \in \mathbb{N}_1$ , we establish

$$X_3 \leq_{st} X_4 \quad (11)$$

by identification of the pgfs. Given (5), we have

$$\eta_1^{\tau^*}(t \mathbf{1}_{1\text{dsc}(1)}) = t(1 - \alpha + \alpha t)^{d-2} = \psi(t, t, \alpha, 1) \times (1 - \alpha + \alpha t)^{d-3}; \quad (12)$$

$$\eta_2^{\tau^*}(t \mathbf{1}_{2\text{dsc}(2)}) = t(1 - \alpha + \alpha t(1 - \alpha + \alpha t)^{d-3}) = \psi(t(1 - \alpha + \alpha t)^{d-3}, t, \alpha, 1), \quad (13)$$

for  $t \in [-1, 1]$ . Therefore, as in (11), it follows that  $H_2^{\tau^*} \leq_{st} H_1^{\tau^*}$ , leading to  $M^{<2>} \leq_{cx} M^{<1>}$  by Theorem 3 allowing to conclude  $\mathcal{T}^{<2>} \leq_{sha} \mathcal{T}^{<1>}$ . Shifting the focus to  $\mathcal{T}^{<2>}$  and  $\mathcal{T}^{<3>}$ , we establish a stochastic dominance relation between  $H_1^{\tau^{**}}$  and  $H_3^{\tau^{**}}$ , with subtree  $\tau^{**}$  having vertices  $\mathcal{V}^{**} = \mathcal{V} \setminus \{4\}$ , in order to apply Theorem 3. Indeed, the two structures only differ by the anchoring position of vertex 4. From (5), we obtain

$$\eta_1^{\tau^{**}}(t \mathbf{1}_{1\text{dsc}(1)}) = t(1 - \alpha + \alpha t)^{d-4}(1 - \alpha t(1 - \alpha t)) = (1 - \alpha + \alpha t)^{d-4} \psi^{(2)}(t, t, \alpha, 1); \quad (14)$$

$$\eta_3^{\tau^{**}}(t \mathbf{1}_{3\text{dsc}(3)}) = t(1 - \alpha + \alpha t(1 - \alpha t((1 - \alpha + \alpha t)^{d-4}))) = \psi^{(2)}(t(1 - \alpha + \alpha t)^{d-4}, t, \alpha, 1), \quad (15)$$

for  $t \in [-1, 1]$ . Given (11), we draw the same conclusions as above and establish  $H_3^{\tau^{**}} \leq_{st} H_1^{\tau^{**}}$ , allowing to conclude that  $M^{<3>} \leq_{cx} M^{<2>}$  by Theorem 3. Hence,  $\mathcal{T}^{<3>} \leq_{sha} \mathcal{T}^{<2>}$ . We repeat these steps until the star has been entirely rearranged as a series tree. The comparing pattern of (12) against (13), and of (14) against (15), indeed reissues at each step, due to the recursiveness of  $\eta_v^{\tau^*}$ .  $\square$

In Appendix D, we provide Hasse diagrams for posets  $(\Omega_{\mathcal{T}}^{(d)}, \leq_{sha})$ , where  $\Omega_{\mathcal{T}}^{(d)}$  is the finite set of all trees comprising  $d$  vertices,  $d \in \{4, \dots, 9\}$ . The diagrams were devised from multiple applications of Theorem 3, considering every combination of trees. Two trees may not be comparable if they either differ by the positions of more than one vertex or if the condition  $H_v^{\tau^*} \leq_{st} H_w^{\tau^*}$  is not satisfied. Notice that the Hasse diagram is not upward planar starting with  $d = 8$ . This coincides with the first occurrences of shapes not being comparable because the condition  $H_v^{\tau^*} \leq_{st} H_w^{\tau^*}$  is not met. Also,  $(\Omega_{\mathcal{T}}, \leq_{sha})$  is not a lattice: some pair of trees have more than one supremum, and others more than one infimum, as observed in the Hasse diagram of  $(\Omega_{\mathcal{T}}^{(9)}, \leq_{sha})$ . The star acts as maximal element and the series tree as minimal element of the subset of  $d$ -vertex trees,  $d \in \{4, \dots, 9\}$ .

The criterion  $H_v^{\tau^*} \leq_{st} H_w^{\tau^*}$  cannot be omitted in Theorem 3: even if two trees differ by the anchoring position of only one vertex, they may not be comparable under  $\leq_{sha}$ . This is illustrated in Example 2.

**Example 2.** Consider  $\mathcal{T}$  and  $\mathcal{T}'$ , the two trees depicted in Figure 4. They differ only by the anchorage of vertex 4:  $\mathcal{E} \setminus \{(2, 4)\} = \mathcal{E}' \setminus \{(3, 4)\}$ . Suppose  $\lambda = 1$  and  $\alpha_e = 0.9$  for every  $e \in \mathcal{E} \cup \mathcal{E}'$ . Subtree  $\tau^*$  is obtained by pruning 4 of either trees. Theorem 3 cannot be applied as  $H_2^{\tau_2^*}$  and  $H_3^{\tau_3^*}$  are not comparable according to the stochastic dominance order. Indeed, one finds  $\Pr(H_2^{\tau_2^*} \leq 1) = 0.01 > 0.001 = \Pr(H_3^{\tau_3^*} \leq 1)$  and  $\Pr(H_2^{\tau_2^*} \leq 2) = 0.0190 < 0.0199 = \Pr(H_3^{\tau_3^*} \leq 2)$ . After computing the values of the pmfs of  $M$  and  $M'$ , we obtain  $\text{TVaR}_{0.23}(M) = 15.4342 < 15.4355 = \text{TVaR}_{0.23}(M')$  and  $\text{TVaR}_{0.97}(M) = 42.3553 > 42.2257 = \text{TVaR}_{0.97}(M')$ , which disrupt the possibility of convex ordering between  $M$  and  $M'$ . Therefore,  $\mathcal{T}$  and  $\mathcal{T}'$  are not comparable under  $\leq_{sha}$ .

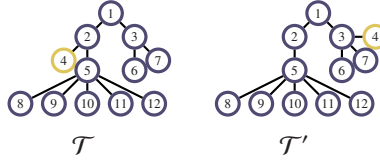


Figure 4: Trees  $\mathcal{T}$  and  $\mathcal{T}'$  of Example 2.

Since the criterion to apply Theorem 3 is the same as the one to apply Theorem 2, but on  $\tau^*$ , one ties the ordering of synecdochic pairs established above to  $\leq_{sha}$  through the following theorem.

**Theorem 4.** Given a tree  $\mathcal{T} = (\mathcal{V}, \mathcal{E})$ , let  $\mathcal{T}^{+i}$ , denote the tree obtained by connecting an additional vertex to  $i$ , for  $i \in \mathcal{V}$ . If  $\mathcal{T}^{+v} \leq_{sha} \mathcal{T}^{+w}$ , for vertices  $v, w \in \mathcal{V}$ , then  $N_v$  is less contributing than  $N_w$  to  $M$  with respect to Definition 2, that is to say  $v$  is less central than  $w$ .

*Proof.* The residual subtree  $\tau^*$  common to both  $\mathcal{T}^{+v}$  and  $\mathcal{T}^{+w}$  is  $\mathcal{T}$ . Hence,  $\mathcal{T}^{+v} \leq_{sha} \mathcal{T}^{+w}$  means  $H_v^{\mathcal{T}^{+v}} \leq_{st} H_w^{\mathcal{T}^{+w}}$ , as the order  $\leq_{sha}$  was induced by Theorem 3. The result follows from Theorem 2.  $\square$

Results facilitating comparison under  $\leq_{sha}$ , such as Corollary 1 and upcoming Corollaries 2, 3 and 4 as well as the Hasse diagrams in Appendix D, thus also serve as tools in the analysis of the joint distribution of synecdochic pairs and related centrality indices. This is exhibited in the following example.

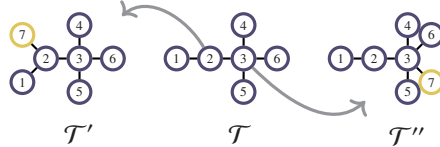


Figure 5: Trees  $\mathcal{T}$ ,  $\mathcal{T}'$  and  $\mathcal{T}''$  from Example 3.

**Example 3.** Consider  $N$  defined on tree  $\mathcal{T}$ , depicted in Figure 5, and with dependence parameters  $\alpha$  such that  $\alpha_e = \alpha$  for every  $e \in \mathcal{E}$ . If one were to add a vertex by connecting it to 2, they would obtain tree  $\mathcal{T}'$ ; if one were to add a vertex by connecting it to 3, they would obtain tree  $\mathcal{T}''$ . Now, referring to Figure 12, we see  $\mathcal{T}' \leq_{sha} \mathcal{T}''$ . Hence, returning to  $\mathcal{T}$ , one deduces that  $N_2$  is less contributing than  $N_3$  to  $M$  given Theorem 4.

We provide additional corollaries to Theorem 3, which, similarly to Corollary 1, prove useful to compare trees differing by more than one edge in accordance to  $\leq_{sha}$ . Each one presents a different sequence of iterative manipulations of trees, for which successive applications of Theorem 3 allow to establish the ordering along the sequence.

**Corollary 2.** Let  $\mathcal{T}^{(1)} = (\mathcal{V}, \mathcal{E}^{(1)})$  be a tree such that, to a specific vertex  $w \in \mathcal{V}$ , are connected subtrees as well as  $d_{ray}$  single vertices, which we call ray-like vertices,  $d_{ray} \in \mathbb{N}_1$ . Define  $\{\mathcal{T}^{(k)}, k \in \{2, \dots, d_{ray} - 1\}\} \subseteq \Omega_{\mathcal{T}}$  as the sequence of trees obtained by successively moving ray-like vertices to form a series subtree connected to  $w$ . Assume  $d \geq 4$ . We have the following ordering of trees:

$$\mathcal{T}^{(d_{ray}-1)} \leq_{sha} \mathcal{T}^{(d_{ray}-2)} \leq_{sha} \dots \leq_{sha} \mathcal{T}^{(2)} \leq_{sha} \mathcal{T}^{(1)}.$$

*Proof.* Aiming to compare  $\mathcal{T}^{(k)}$  and  $\mathcal{T}^{(k+1)}$ ,  $k \in \{1, \dots, d_{\text{ray}} - 2\}$ , let  $v$  be the vertex to which the ray-like vertex from  $\mathcal{T}^{(k)}$  anchors itself in  $\mathcal{T}^{(k+1)}$ . We show  $H_v^{\tau_v^*} \leq_{st} H_w^{\tau_w^*}$  when dependence parameters are all  $\alpha$ ,  $\alpha \in [0, 1]$ , with  $\tau^*$  being  $\mathcal{T}^{(k)}$  pruned of that moving ray-like vertex. With  $\psi$  as in (10), we obtain from (5)

$$\eta_v^{\tau_v^*}(t \mathbf{1}_{|v\text{dsc}(v)|}) = \psi^{(k)} \left( t(1 - \alpha + \alpha t)^{d_{\text{ray}} - k - 1} \prod_{j \in \text{sub}} (1 - \alpha + \alpha \eta_j^{\tau_j^*}(t \mathbf{1}_{|j\text{dsc}(j)|}), t, \alpha, 1 \right), \quad (16)$$

and

$$\eta_w^{\tau_w^*}(t \mathbf{1}_{|w\text{dsc}(w)|}) = \psi^{(k)}(t, t, \alpha, 1) \times (1 - \alpha + \alpha t)^{d_{\text{ray}} - k - 1} \prod_{j \in \text{sub}} (1 - \alpha + \alpha \eta_j^{\tau_j^*}(t \mathbf{1}_{|j\text{dsc}(j)|})), \quad (17)$$

with sub denoting the set of vertices by which the generic subtrees are connected to  $v$ . For all  $j \in \text{sub}$ , we have  $\eta_j^{\tau_j^*}(t \mathbf{1}_{|j\text{dsc}(j)|}) = \eta_j^{\tau_j^*}(t \mathbf{1}_{|j\text{dsc}(j)|})$ ,  $t \in [-1, 1]$ , as the children of  $j$  are the same under both rooting. Therefore, from (11), (16) and (17), we deduce  $H_v^{\tau_v^*} \leq_{st} H_w^{\tau_w^*}$ ; hence,  $\mathcal{T}^{(k+1)} \leq_{sha} \mathcal{T}^{(k)}$ ,  $k \in \{1, \dots, d_{\text{ray}} - 2\}$ .  $\square$



Figure 6: Example of a sequence of trees encompassed by Corollary 2. Vertex of interest  $w$  is in blue (dark shade), generic subtrees connected to it are in orange (mid shade), ray-like vertices and the series subtree they form are in yellow (light shade).

We depict in Figure 6 an example of the sequence  $\{\mathcal{T}^{(k)}, k \in \{1, \dots, d_{\text{ray}} - 1\}\}$  induced by the reconstruction of a tree  $\mathcal{T}^{(1)}$ . Corollary 2 should be seen as a generalization of Corollary 1: vertex  $d$  in Figure 3 is a connected subtree while vertices 2 to  $d - 1$  are the ray-like vertices.

**Corollary 3.** Let  $\mathcal{T}^{[1]} = (\mathcal{V}, \mathcal{E}^{[1]})$  be a  $d_{\text{se}}$ -vertex series subtree to which is connected at one end a subtree  $\tau$ ,  $d_{\text{se}} \geq 3$ . Let  $\{l_k, k \in \{1, \dots, d_{\text{se}}\}\}$  label the successive vertices of the series subtree, with  $l_1$  connected to  $\tau$ . Define  $\{\mathcal{T}^{[k]}, k \in \{2, \dots, k_{\text{max}}\}\} \subseteq \Omega_{\mathcal{T}}$ ,  $k_{\text{max}} = \lfloor \frac{d_{\text{se}}}{2} \rfloor$ , as the sequence of trees obtained by anchoring  $\tau$  to  $l_k$  rather than  $l_1$ ,  $k \in \{1, \dots, k_{\text{max}}\}$ . We have the following ordering of trees:

$$\mathcal{T}^{[1]} \leq_{sha} \mathcal{T}^{[2]} \leq_{sha} \dots \leq_{sha} \mathcal{T}^{[k_{\text{max}}-1]} \leq_{sha} \mathcal{T}^{[k_{\text{max}}]}.$$

*Proof.* Let  $\tau^*$  denote the series subtree of interest. We show  $H_{l_k}^{\tau_{l_k}^*} \leq_{st} H_{l_{k+1}}^{\tau_{l_{k+1}}^*}$  for all  $k \in \{1, \dots, k_{\text{max}} - 1\}$  when dependence parameters are all  $\alpha$ ,  $\alpha \in (0, 1)$ . We remark that, rooting on  $l_{k+1}$ ,  $\text{ch}(l_k) = \{l_{k-1}\}$ ; meanwhile rooting on  $l_k$ ,  $\text{ch}(l_k) = \{l_{k-1}, l_{k+1}\}$ . Also, from (5),  $\eta_{l_{k+2}}^{\tau_{l_{k+2}}^*}(t \mathbf{1}_{|l_{k+2}\text{dsc}(l_{k+2})|}) = \eta_{l_{k+2}}^{\tau_{l_{k+2}}^*}(t \mathbf{1}_{|l_{k+2}\text{dsc}(l_{k+2})|})$  as the children of  $l_{k+2}$  are the same under both rootings, leading to

$$\begin{aligned} \eta_{l_k}^{\tau_{l_k}^*}(t \mathbf{1}_{|l_k\text{dsc}(l_k)|}) &= \eta_{l_k}^{\tau_{l_{k+1}}^*}(t \mathbf{1}_{|l_k\text{dsc}(l_k)|}) \times (1 - \alpha + \alpha t(1 - \alpha + \alpha \eta_{l_{k+2}}^{\tau_{l_{k+2}}^*}(t \mathbf{1}_{|l_{k+2}\text{dsc}(l_{k+2})|}))) \\ &= (1 - \alpha) \eta_{l_k}^{\tau_{l_{k+1}}^*}(t \mathbf{1}_{|l_k\text{dsc}(l_k)|}) + \alpha t \eta_{l_k}^{\tau_{l_{k+1}}^*}(t \mathbf{1}_{|l_k\text{dsc}(l_k)|}) (1 - \alpha + \alpha \eta_{l_{k+2}}^{\tau_{l_{k+2}}^*}(t \mathbf{1}_{|l_{k+2}\text{dsc}(l_{k+2})|})). \end{aligned} \quad (18)$$

Next, directly from (5), one obtains

$$\begin{aligned} \eta_{l_{k+1}}^{\tau_{l_{k+1}}^*}(t \mathbf{1}_{|l_{k+1}\text{dsc}(l_{k+1})|}) &= t \times (1 - \alpha + \alpha \eta_{l_k}^{\tau_{l_{k+1}}^*}(t \mathbf{1}_{|l_k\text{dsc}(l_k)|})) \times (1 - \alpha + \alpha \eta_{l_{k+2}}^{\tau_{l_{k+2}}^*}(t \mathbf{1}_{|l_{k+2}\text{dsc}(l_{k+2})|})) \\ &= (1 - \alpha) t (1 - \alpha + \alpha \eta_{l_{k+2}}^{\tau_{l_{k+2}}^*}(t \mathbf{1}_{|l_{k+2}\text{dsc}(l_{k+2})|})) + \alpha t \eta_{l_k}^{\tau_{l_{k+1}}^*}(t \mathbf{1}_{|l_k\text{dsc}(l_k)|}) (1 - \alpha + \alpha \eta_{l_{k+2}}^{\tau_{l_{k+2}}^*}(t \mathbf{1}_{|l_{k+2}\text{dsc}(l_{k+2})|})). \end{aligned} \quad (19)$$

We note  $\eta_{l_k}^{\tau_{l_{k+1}}^*}(t \mathbf{1}_{|l_k\text{dsc}(l_k)|}) = \eta_{l_{d_{\text{se}}+1-k}}^{\tau_{l_{k+1}}^*}(t \mathbf{1}_{|l_{d_{\text{se}}+1-k}\text{dsc}(l_{d_{\text{se}}+1-k})|})$  by the symmetry of the series subtree. Since  $l_{d_{\text{se}}+1-k} \in \{l_{k+2}\} \cup \text{dsc}(l_{k+2})$  under rooting  $l_{k+1}$ , for  $k \leq k_{\text{max}}$ , the pgfs in (18) and (19) indicate that  $H_{l_k}^{\tau_{l_k}^*} \leq_{st} H_{l_{k+1}}^{\tau_{l_{k+1}}^*}$ . Hence,  $\mathcal{T}^{[k]} \leq_{sha} \mathcal{T}^{[k+1]}$  according to Theorem 3.  $\square$

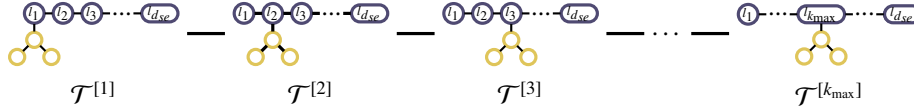


Figure 7: Example of a sequence of trees encompassed by Corollary 3. The series subtree is in blue (dark shade) while the generic subtree  $\tau$  is in yellow (light shade).

We depict in Figure 7 an example of the sequence  $\{\mathcal{T}^{[k]}, k \in \{1, \dots, k_{\max}\}\}$  induced by a tree  $\mathcal{T}^{[1]}$ .

**Corollary 4.** Consider  $d_{\text{beam}}, d_{\text{ray}} \in \mathbb{N}_1$ , with  $d_{\text{beam}} + d_{\text{ray}} \leq d$ , assuming  $d \geq 4$ . Let  $\{\mathcal{T}^{(m;n)}, m, n \in \mathbb{N} : m + n = d_{\text{ray}}\} \subseteq \Omega_{\mathcal{T}}$  be a sequence of trees such that to a  $d_{\text{beam}}$ -vertex series subtree, which we call the beam subtree and whose vertices are labelled  $\{l_k, k \in \{1, \dots, d_{\text{beam}}\}\}$ , we connect  $m$  vertices to an end and  $n$  vertices to the other end. Additional subtrees may be connected to the beam subtree, in a symmetric manner: for a subtree connected to  $l_k$ , an identical subtree is connected to  $l_{d_{\text{beam}}-k}$ ,  $k \in \{1, \dots, \lfloor \frac{d_{\text{beam}}}{2} \rfloor\}$ . For  $m_1, n_1, m_2, n_2 \in \mathbb{N}$  such that  $m_1 + n_1 = m_2 + n_2$ , if  $|m_1 - n_1| \leq |m_2 - n_2|$ , then  $\mathcal{T}^{(m_1;n_1)} \leq_{\text{sha}} \mathcal{T}^{(m_2;n_2)}$ .

*Proof.* Let  $\tau^* = \mathcal{T}^{(a^*;b)}$ , with  $a^* = a - 1$ . We establish stochastic dominance ordering between  $H_{l_1}^{\tau^*}$  and  $H_{l_{d_{\text{beam}}}}^{\tau^*}$  with all dependence parameters being  $\alpha$ ,  $\alpha \in (0, 1)$ . Let us denote by  $\tau''$  the beam subtree with the additional subtrees connected to it. From (5), we have

$$\eta_{l_1}^{\tau^*}(t \mathbf{1}_{|l_1 \text{ dsc}(l_1)|}) = (1 - \alpha + \alpha t)^{a^*} \underbrace{\eta_{l_1}^{\tau''}(t, \dots, t(1 - \alpha + \alpha t)^b, \dots, t, t)}_{\text{position } l_{d_{\text{beam}}}}; \quad (20)$$

$$\eta_{l_{d_{\text{beam}}}}^{\tau^*}(t \mathbf{1}_{|l_{d_{\text{beam}}} \text{ dsc}(l_{d_{\text{beam}}})|}) = (1 - \alpha + \alpha t)^b \underbrace{\eta_{l_{d_{\text{beam}}}}^{\tau''}(t, t, \dots, t(1 - \alpha + \alpha t)^{a^*}, \dots, t, t)}_{\text{position } l_1}; \quad (21)$$

for  $t \in [-1, 1]$ . By the symmetry of  $\tau''$ , one has  $\eta_{l_1}^{\tau''}(t \mathbf{1}_{|l_1 \text{ dsc}(l_1)|}) = \eta_{l_{d_{\text{beam}}}}^{\tau''}(t \mathbf{1}_{|l_{d_{\text{beam}}} \text{ dsc}(l_{d_{\text{beam}}})|})$ . Therefore, from (20) and (21), we infer that  $H_{l_1}^{\tau^*} \leq_{st} H_{l_{d_{\text{beam}}}}^{\tau^*}$  as long as  $a^* \leq b$ , and vice-versa. Consequently,  $\mathcal{T}^{(a^*;b+1)} \leq_{\text{sha}} \mathcal{T}^{(a^*;b)}$  if  $a^* \leq b$ , and  $\mathcal{T}^{(a^*;b+1)} \leq_{\text{sha}} \mathcal{T}^{(a^*;b)}$  if  $a^* \geq b$ , according to Theorem 3. The result follows from the transitivity of  $\leq_{\text{sha}}$ .  $\square$

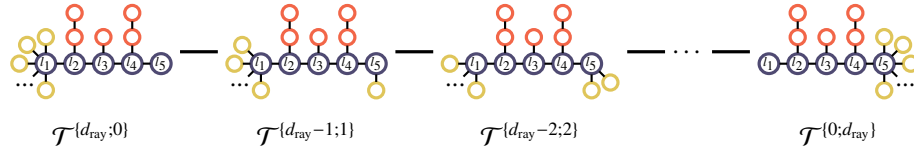
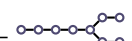


Figure 8: Example of a sequence of trees encompassed by Corollary 4. The moving vertices are in yellow (light shade), the beam subtree is in blue (dark shade), and the additional subtrees attached to it are in orange (mid shade).

We depict in Figure 8 an example of a sequence  $\{\mathcal{T}^{(m;n)}, m, n \in \mathbb{N} : m + n = d_{\text{ray}}\}$  with  $d_{\text{beam}} = 5$ , as encompassed by Corollary 4. Combining the use of Corollaries 2, 3 and 4 offers wide possibilities of comparison, as exhibited in the following example.

**Example 4.** Assuming a set of  $d = 9$  vertices, let  $\mathcal{T} =$   and  $\mathcal{T}' =$  . By first applying Corollary 4, then Corollary 2, and finally Corollary 3, as shown in Figure 9, we establish  $\mathcal{T} \leq_{\text{sha}} \mathcal{T}'$ . Note that this ordering agrees with the Hasse diagram depicted in Figure 12.  $\square$

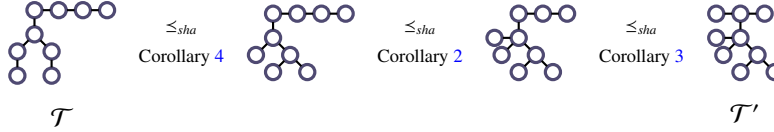


Figure 9: A combined use of Corollaries 2, 3 and 4 to order using  $\leq_{sha}$

Bases of comparison for trees already exist in the (spectral) graph theory literature; however, they have not been explored, to our knowledge, in the context of MRFs. In this section, we look at a few of them and provide discussion and examples showing their distinctiveness with  $\leq_{sha}$ .

The *degree* of a vertex is the number of edges connected to it. Let  $\pi^{\mathcal{T}}$  denote the decreasingly ordered vector of degrees of a tree  $\mathcal{T}$ . Trees may be gathered in categories following their respective vector  $\pi^{\mathcal{T}}$ . Ordering between two trees of different categories, say  $\mathcal{T}$  and  $\mathcal{T}'$ , is established if  $\sum_{i=1}^k \pi_i^{\mathcal{T}} \leq \sum_{i=1}^k \pi_i^{\mathcal{T}'}$ , for all  $k \in \{1, \dots, d\}$ . Such a comparison is called *majorization*; see [Marshall et al., 2011]. Thus categorizing and comparing trees have been prominently studied in the context of spectral graph theory, notably in [Liu et al., 2009] and subsequent work. Majorization of vectors of degrees does not produce the order given by  $\leq_{sha}$ . On one hand, trees having the same  $\pi^{\mathcal{T}}$  may still be ordered according to  $\leq_{sha}$ ;  $\mathcal{T}^{[2]}$  and  $\mathcal{T}^{[3]}$  of Figure 7 are an example. On the other hand, a tree whose vector of degrees majorizes another's may be incomparable according to  $\leq_{sha}$ ; take  $\mathcal{T}$  and  $\mathcal{T}'$  of Figure 4 as an example.

Another ground of comparison of trees is the algebraic connectivity, introduced in [Fiedler, 1973]. Algebraic connectivity corresponds to the second smallest eigenvalue of a graph's Laplacian matrix, defined as the identity matrix minus the adjacency matrix; one may consult [Grone and Merris, 1987] for further insight in the context of trees. Comparing with respect to  $\leq_{sha}$  is distinct than ordering trees according to algebraic connectivity as investigated in [Grone and Merris, 1990]. A glance at Table 1 therein and Figure 12 for  $d = 7$  allows to visualize the distinction.

Spectral graph theory provides other means of comparison of trees, notably employing the spectral radius or the Estrada index. Denote the set of eigenvalues of the adjacency matrix of a graph by  $\{\mu_i, i \in \{1, \dots, d\}\}$ . Then, the spectral radius of that graph is given by  $\rho_{\text{spec}}(\mathcal{T}) = \max_{i=1}^d \mu_i$  and its Estrada index by  $EE(\mathcal{T}) = \sum_{i=1}^d e^{\mu_i}$ . One may consult [Gutman et al., 2011] for a review on the Estrada index. Exhaustive computations showed that, for  $d \in \{4, \dots, 8\}$ ,  $\mathcal{T} \leq_{sha} \mathcal{T}'$  yields  $\rho_{\text{spec}}(\mathcal{T}) \leq \rho_{\text{spec}}(\mathcal{T}')$  and  $EE(\mathcal{T}) \leq EE(\mathcal{T}')$ . This remains mostly true for larger number of vertices, but exceptions surface, as exhibited in Example 5. Moreover, referring to Figure 12, we observe  $\text{---} \leq_{sha} \text{---}$ , while both trees' adjacency matrix have the same eigenvalues: they are cospectral. Tools from spectral graph theory, even apart from the spectral radius and the Estrada index, are therefore not sufficient to entirely describe the comparison dynamics at play in  $(\Omega_{\mathcal{T}}, \leq_{sha})$ .

**Example 5.** Consider trees  $\mathcal{T}$  and  $\mathcal{T}'$  depicted in Figure 10. They differ only by the anchorage of vertex 9, connected to 3 in one case and to 7 in the other. From (5), for  $\tau^*$  the subtree obtained by pruning 9, we have

$$\begin{aligned} \eta_3^{\tau^*}(t \mathbf{1}_8) &= t(1 - \alpha + \alpha t[1 - \alpha + \alpha t])(1 - \alpha + \alpha t[1 - \alpha + \alpha t\{1 - \alpha + \alpha t(1 - \alpha + \alpha t)\}]); \\ \eta_7^{\tau^*}(t \mathbf{1}_8) &= t\{1 - \alpha + \alpha t\}\{1 - \alpha + \alpha t(1 - \alpha + \alpha t)(1 - \alpha + \alpha t[1 - \alpha + \alpha t\{1 - \alpha + \alpha t(1 - \alpha + \alpha t)\}])\}, \end{aligned}$$

which, when developed, indicates  $H_7^{\tau^*} \leq_{st} H_3^{\tau^*}$ . Hence,  $\mathcal{T} \leq_{sha} \mathcal{T}'$  by Theorem 3, although  $\rho_{\text{spec}}(\mathcal{T}) = 2.0840 > 2.0743 = \rho_{\text{spec}}(\mathcal{T}')$  and  $EE(\mathcal{T}) = 19.4594 > 19.4591 = EE(\mathcal{T}')$ .

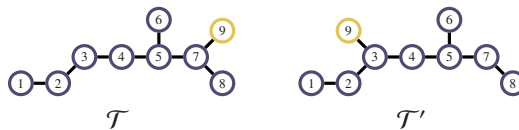


Figure 10: Trees  $\mathcal{T}$  and  $\mathcal{T}'$  from Example 5

In [Csikvari, 2010], the author introduces a transformation on trees, the *generalized tree shift*, and designs a poset according to this transformation. This idea was further explored in [Csikvari, 2013]. According to this poset, a tree

$\mathcal{T}$  precedes another tree  $\mathcal{T}'$ , which we denote  $\mathcal{T} \leq_{gts} \mathcal{T}'$ , if  $\mathcal{T}'$  is the image of a generalized tree shift on  $\mathcal{T}$ . This gives the poset  $(\Omega_{\mathcal{T}}, \leq_{gts})$ . Roughly,  $(\Omega_{\mathcal{T}}, \leq_{gts})$  is coarser than  $(\Omega_{\mathcal{T}}, \leq_{sha})$ , that is, many comparisons with respect to  $\leq_{sha}$  cannot be established according to  $\leq_{gts}$ . Corollaries 3 and 4 provide evidence of that: in sequences of trees encompassed by either, intermediary trees cannot be obtained from one another through a generalized tree shift. Conversely, most generalized tree shifts are reproducible through successive applications of Theorem 3, and thus, in most cases,  $\mathcal{T} \leq_{gts} \mathcal{T}'$  implies  $\mathcal{T} \leq_{sha} \mathcal{T}'$ . Evidence suggests this is not true in general, however. Figure 11 depicts two trees,  $\mathcal{T}$  and  $\mathcal{T}'$ , such that  $\mathcal{T}'$  is the result of a generalized tree shift on  $\mathcal{T}$ , meaning  $\mathcal{T} \leq_{gts} \mathcal{T}'$ . However, for every  $\tau^*$  obtained by pruning one of the subtrees in orange (mid shade) or yellow (light shade) from  $\mathcal{T}$ , the condition  $H_v^{\tau^*} \leq_{st} H_w^{\tau^*}$  is not met, suggesting incomparability according to  $\leq_{sha}$  since no iterative reconstruction seems to permit comparison. It still seems reasonable to believe  $M \leq_{cx} M'$ , with both respectively defined on  $\mathcal{T}$  and  $\mathcal{T}'$ , and their dependence parameters identical for every edge. Figure 11 hence provides an example illustrating that the need for trees to differ only by one edge to meet the conditions of Theorem 3 may be limiting. Further results on convex orderings could possibly refine the poset  $(\Omega_{\mathcal{T}}, \leq_{sha})$  by permitting comparisons unreachable with the sole result of Theorem 3 and iterative reconstructions. Recall that the condition  $H_v^{\tau^*} \leq_{st} H_w^{\tau^*}$  is simply sufficient, not necessary. In that prospect, the implication  $\mathcal{T} \leq_{gts} \mathcal{T}' \implies \mathcal{T} \leq_{sha} \mathcal{T}'$  could become valid.

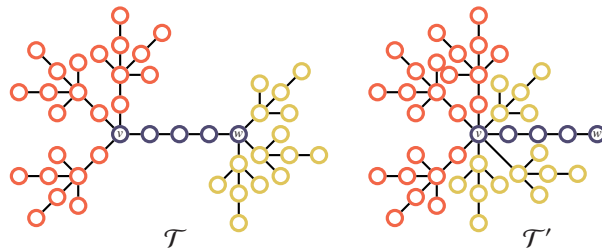


Figure 11: A generalized tree shift from  $\mathcal{T}$  to  $\mathcal{T}'$

## 5 Conclusion

The main contributions of this paper revolve around stochastic orderings in the context of the family MPMRF. Within a given tree, we have established supermodular orderings of synecdochic pairs, the pair given by a component of a random vector and its sum. This was done to assess if a component of the MRF contributes less or more than another to the sum, depending on its corresponding vertex's position. Our findings on the ordering of synecdochic pairs have also found repercussions for allocation-related quantities, which invited their consideration as centrality indices. These findings were also key to deriving the result that allowed for establishing convex ordering of sums of MRFs defined on trees of different shapes. To thoroughly explore this latter result, we have designed a new partial order on trees and examined it exhaustively. This examination was done through the conception of Hasse diagrams, tools facilitating comparison along sequences of trees, and a discussion stemming from spectral graph theory on its relation to other poset of trees. Moreover, we have shown that the two stochastic orderings,  $(N_v, M) \leq_{sm} (N_w, M)$  and  $M \leq_{cx} M'$ , were two sides of the same coin, both linked through the condition  $H_v^{\tau^*} \leq_{st} H_w^{\tau^*}$ ,  $v, w \in \mathcal{V}$ . Our acquired comprehension of the poset  $(\Omega_{\mathcal{T}}, \leq_{sha})$  thus transposes to both.

One could dive deeper into the analysis of the poset  $(\Omega_{\mathcal{T}}, \leq_{sha})$  using graph-theoretic machinery. [Li and Yu, 2021] furthered the understanding of [Csikvári, 2010]'s poset, revealing results relating to the Wiener index and tree invariants' polynomials; likewise, we suspect more could be uncovered about  $(\Omega_{\mathcal{T}}, \leq_{sha})$  in connection with (spectral) graph theory. [Barghi and DeFord, 2024] discusses, among other things, the ordering of trees induced by some global closeness index and notably proves that the series tree [star tree] acts as its minimum [maximum] element. Further analytical results on that ordering could perhaps, given  $\leq_{sha}$ 's underlying relation to closeness, connect both in the same fashion that the ordering of synecdochic pairs from Theorem 2 connected to centrality indices in Proposition 1. Ergo, the conclusions of [Barghi and DeFord, 2024]'s comparative study could then transpose to  $\leq_{sha}$ .

## A Proof of Theorem 2

The proof comprises two parts. In the first part, we dissect the joint distributions of  $(N_v, M)$  and  $(N_w, M)$  to provide an alternative stochastic representation of both vectors. In the second part, we rely on the mass transfer characterization of supermodular ordering given by [Meyer and Strulovici, 2015] to establish comparison using this alternative representation. For a discussion on the relation tying stochastic orders to mass transfer, see [Müller, 2013]. Appendix C of [Ansari and Rüschemdorf, 2024] also relies on that characterization and provides further insight. Theorem 7 of [Côté et al., 2024] provides the expression of the pgf of  $M$ . Considering first  $v$  as a root, we have

$$\mathcal{P}_M(t_m) = e^{\lambda(d - \sum_{e \in \mathcal{E}} \alpha_e) \left( \left( \sum_{j \in \mathcal{V}} \frac{1 - \alpha(\text{par}(j), j)}{d - \sum_{e \in \mathcal{E}} \alpha_e} \eta_j^{\mathcal{T}_v}(t \mathbf{1}_{\text{jdisc}(j)}) \right) - 1 \right)} \quad (22)$$

$$\begin{aligned} &= e^{\lambda \left( \eta_v^{\mathcal{T}_v}(t_m \mathbf{1}_{\text{vdisc}(v)}) + \sum_{j \in \mathcal{V} \setminus \{v\}} (1 - \alpha) \eta_j^{\mathcal{T}_v}(t_m \mathbf{1}_{\text{jdisc}(j)}) \right) - \lambda d (1 - \alpha)} \\ &= e^{\lambda \left( \sum_{k=0}^{\infty} \left( p_{H_v^{\mathcal{T}_v}}(k) + \sum_{j \in \mathcal{V} \setminus \{v\}} (1 - \alpha) p_{H_j^{\mathcal{T}_v}}(k) \right) t_m^k \right) - \lambda d (1 - \alpha)}, \quad t_m \in [-1, 1]. \end{aligned} \quad (23)$$

For notation purposes, let us define  $\zeta_k = p_{H_v^{\mathcal{T}_v}}(k) + \sum_{j \in \mathcal{V} \setminus \{v\}} (1 - \alpha) p_{H_j^{\mathcal{T}_v}}(k)$ ,  $k \in \mathbb{N}$ . Meanwhile, selecting  $w$  instead as the root, we also have

$$\mathcal{P}_M(t_m) = e^{\lambda \left( \sum_{k=0}^{\infty} \left( p_{H_w^{\mathcal{T}_w}}(k) + \sum_{j \in \mathcal{V} \setminus \{w\}} (1 - \alpha) p_{H_j^{\mathcal{T}_w}}(k) \right) t_m^k \right) - \lambda d (1 - \alpha)}, \quad t_m \in [-1, 1]. \quad (24)$$

Since the choice of the root has no impact on the joint distribution of  $N$  (Theorem 2 of [Côté et al., 2024]) and due to the uniqueness of pgfs, the relation  $\zeta_k = p_{H_w^{\mathcal{T}_w}}(k) + \sum_{j \in \mathcal{V} \setminus \{w\}} (1 - \alpha) p_{H_j^{\mathcal{T}_w}}(k)$  is valid for  $k \in \mathbb{N}$  by comparing (23) and (24). We derive the joint pgfs of  $(N_v, M)$  and  $(N_w, M)$  from the joint pgf of  $N$  using Theorem 2.3 of [Blier-Wong et al., 2022] as follows

$$\mathcal{P}_{N_v, M}(t_v, t_m) = \mathcal{P}_N(t_m, t_m, \dots, \underbrace{t_v t_m}_{\text{position } v}, \dots, \underbrace{t_m}_{\text{position } w}, \dots, t_m, t_m); \quad (25)$$

$$\mathcal{P}_{N_w, M}(t_w, t_m) = \mathcal{P}_N(t_m, t_m, \dots, \underbrace{t_m}_{\text{position } v}, \dots, \underbrace{t_w t_m}_{\text{position } w}, \dots, t_m, t_m), \quad (26)$$

for  $t_v, t_w, t_m \in [-1, 1]$ . From the expression of the joint pgf in (4), choosing  $v$  as the root, relation (25) grants

$$\begin{aligned} \mathcal{P}_{N_v, M}(t_v, t_m) &= e^{\lambda(t_v \eta_v^{\mathcal{T}_v}(t_m \mathbf{1}_{\text{vdisc}(v)}) - 1)} \times \prod_{j \in \mathcal{V} \setminus \{v\}} e^{\lambda(1 - \alpha) \left( \eta_j^{\mathcal{T}_v}(t_m \mathbf{1}_{\text{jdisc}(j)}) - 1 \right)} \\ &= e^{\lambda \left( \sum_{k=1}^{\infty} p_{H_v^{\mathcal{T}_v}}(k) t_v t_m^k + \sum_{k=1}^{\infty} \sum_{j \in \mathcal{V} \setminus \{v\}} (1 - \alpha) p_{H_j^{\mathcal{T}_v}}(k) t_m^k \right) - \lambda d (1 - \alpha)} \\ &= e^{\lambda \left( \sum_{k=1}^{\infty} p_{H_v^{\mathcal{T}_v}}(k) t_v t_m^k + \sum_{k=1}^{\infty} (\zeta_k - p_{H_v^{\mathcal{T}_v}}(k)) t_m^k \right) - \lambda d (1 - \alpha)}, \quad t_v, t_m \in [-1, 1]. \end{aligned} \quad (27)$$

Similarly, choosing  $w$  as the root and following the same steps, (26) yields

$$\mathcal{P}_{N_w, M}(t_w, t_m) = e^{\lambda \left( \sum_{k=1}^{\infty} p_{H_w^{\mathcal{T}_w}}(k) t_w t_m^k + \sum_{k=1}^{\infty} (\zeta_k - p_{H_w^{\mathcal{T}_w}}(k)) t_m^k \right) - \lambda d (1 - \alpha)}, \quad t_w, t_m \in [-1, 1]. \quad (28)$$

To alleviate the notation for the remaining of the proof, define  $a_k = p_{H_v^{\mathcal{T}_v}}(k)$  and  $b_k = p_{H_w^{\mathcal{T}_w}}(k)$ . Also, let  $r = \sum_{k=0}^{\infty} (b_k - a_k) \mathbb{1}_{\{a_k \leq b_k\}} = \sum_{k=0}^{\infty} (a_k - b_k) \mathbb{1}_{\{a_k \geq b_k\}}$ . One may note that  $r$  corresponds to the total variation distance between  $H_v^{\mathcal{T}_v}$  and  $H_w^{\mathcal{T}_w}$ . Consider a random variable  $Y$  whose pgf is given by

$$\mathcal{P}_Y(t) = e^{(\lambda d (1 - \alpha) - \lambda^* r) \left( \frac{1}{d(1 - \alpha) - (1 + r)} \sum_{k=0}^{\infty} (\zeta_k - a_k - (b_k - a_k) \mathbb{1}_{\{a_k \leq b_k\}}) t^k - 1 \right)}, \quad t \in [-1, 1], \quad (29)$$

where  $\lambda^* = \lambda(1 + r)$ . From the definitions of  $a_k$ ,  $b_k$  and  $\zeta_k$ , one directly sees  $\zeta_k - a_k \geq 0$  and  $\zeta_k - b_k \geq 0$  for every  $k \in \mathbb{N}$ . Thus, the quantity  $\zeta_k - a_k - (b_k - a_k) \mathbb{1}_{\{a_k \leq b_k\}}$ , which is equal to  $\zeta_k - b_k - (a_k - b_k) \mathbb{1}_{\{a_k \geq b_k\}}$ , is nonnegative for every  $k \in \mathbb{N}$ . The pgf in (29) is thus, indeed, a valid pgf.

The joint pgf in (27) then becomes

$$\begin{aligned}\mathcal{P}_{N_v, M}(t_v, t_m) &= e^{\lambda(\sum_{k=0}^{\infty} a_k t_v^k + \sum_{k=0}^{\infty} (\zeta_k - a_k) t_m^k) - \lambda d(1-\alpha)} \\ &= e^{\lambda(\sum_{k=0}^{\infty} a_k t_v^k + \sum_{k=0}^{\infty} (b_k - a_k) \mathbb{1}_{\{a_k \leq b_k\}} t_m^k + \sum_{k=0}^{\infty} (\zeta_k - a_k - (b_k - a_k) \mathbb{1}_{\{a_k \leq b_k\}}) t_m^k) - \lambda d(1-\alpha)} \\ &= e^{\lambda^* (\frac{1}{1+r} (\sum_{k=0}^{\infty} a_k t_v^k + \sum_{k=0}^{\infty} (b_k - a_k) \mathbb{1}_{\{a_k \leq b_k\}} t_m^k) - 1)} \times \mathcal{P}_Y(t_m), \quad t_v, t_m \in [-1, 1].\end{aligned}\quad (30)$$

Likewise, (28) becomes

$$\mathcal{P}_{N_w, M}(t_w, t_m) = e^{\lambda^* (\frac{1}{1+r} (\sum_{k=0}^{\infty} b_k t_w^k + \sum_{k=0}^{\infty} (a_k - b_k) \mathbb{1}_{\{a_k \geq b_k\}} t_m^k) - 1)} \times \mathcal{P}_Y(t_m) \quad t_w, t_m \in [-1, 1], \quad (31)$$

since  $\zeta_k - a_k - (b_k - a_k) \mathbb{1}_{\{a_k \leq b_k\}} = \zeta_k - b_k - (a_k - b_k) \mathbb{1}_{\{a_k \geq b_k\}}$  for every  $k \in \mathbb{N}$ . Next, let  $(\check{I}_v, \check{H}_v)$  and  $(\check{I}_w, \check{H}_w)$  be vectors of random variables whose joint pgfs are respectively given by

$$\mathcal{P}_{\check{I}_v, \check{H}_v}(t_v, t_m) = \frac{1}{1+r} \left( \sum_{k=0}^{\infty} a_k t_v^k + \sum_{k=0}^{\infty} (b_k - a_k) \mathbb{1}_{\{a_k \leq b_k\}} t_m^k \right); \quad (32)$$

$$\mathcal{P}_{\check{I}_w, \check{H}_w}(t_w, t_m) = \frac{1}{1+r} \left( \sum_{k=0}^{\infty} b_k t_w^k + \sum_{k=0}^{\infty} (a_k - b_k) \mathbb{1}_{\{a_k \geq b_k\}} t_m^k \right), \quad (33)$$

for  $t_v, t_w, t_m \in [-1, 1]$ . From (32) and (33), we note  $\mathcal{P}_{\check{I}_v, \check{H}_v}(t, 1) = \mathcal{P}_{\check{I}_w, \check{H}_w}(t, 1)$ , for all  $t \in [-1, 1]$ . Hence,  $\check{I}_v \stackrel{d}{=} \check{I}_w$ ; they indeed both follow a Bernoulli distribution of parameter  $\frac{1}{1+r}$ . We similarly deduce  $\check{H}_v \stackrel{d}{=} \check{H}_w$ . Finally, let  $\check{N}$  be a random variable following a Poisson distribution of parameter  $\lambda^*$ . Its pgf is given by

$$\mathcal{P}_{\check{N}}(t) = e^{\lambda^*(t-1)}, \quad t \in [-1, 1]. \quad (34)$$

Using (29), (32), (33) and (34), we rewrite (30) and (31) as

$$\mathcal{P}_{N_v, M}(t_v, t_m) = \mathcal{P}_{\check{N}} \left( \mathcal{P}_{\check{I}_v, \check{H}_v}(t_v, t_m) \right) \times \mathcal{P}_Y(t_m); \quad (35)$$

$$\mathcal{P}_{N_w, M}(t_w, t_m) = \mathcal{P}_{\check{N}} \left( \mathcal{P}_{\check{I}_w, \check{H}_w}(t_w, t_m) \right) \times \mathcal{P}_Y(t_m), \quad (36)$$

for  $t_v, t_w, t_m \in [-1, 1]$ . Hence, given the uniqueness of joint pgfs, we deduce from (35) and (36)

$$(N_v, M) \stackrel{d}{=} \left( \sum_{i=1}^{\check{N}} \check{I}_{v,i}, \sum_{i=1}^{\check{N}} \check{H}_{v,i} + Y \right); \quad (N_w, M) \stackrel{d}{=} \left( \sum_{i=1}^{\check{N}} \check{I}_{w,i}, \sum_{i=1}^{\check{N}} \check{H}_{w,i} + Y \right), \quad (37)$$

where  $\{(\check{I}_{v,i}, \check{H}_{v,i}), i \in \mathbb{N}_1\}$  and  $\{(\check{I}_{w,i}, \check{H}_{w,i}), i \in \mathbb{N}_1\}$  are sequences of independent vectors of random variables identically distributed to  $(\check{I}_v, \check{H}_v)$  and  $(\check{I}_w, \check{H}_w)$  respectively, and where  $\check{N}$  and  $Y$  are independent random variables, also independent of the two sequences. Relations in (37) provide the sought alternative representations.

The second part of the demonstration rests on Theorem 1 of [Meyer and Strulovici, 2015]. Before continuing, let us present it in a bivariate context, in details and without proof, as follows.

**Theorem 1 of [Meyer and Strulovici, 2015].** Consider two vectors of random variables,  $X$  and  $X'$ , taking values in  $\mathbb{N}^2$  with joint pmfs  $p_X$  and  $p_{X'}$ . Then,  $X \leq_{sm} X'$  if and only if there exist nonnegative coefficients  $(\gamma_\beta)_{\beta \in \mathbf{\beta}}$  such that

$$p_{X'}(\mathbf{x}) = p_X(\mathbf{x}) + \sum_{\beta \in \mathbf{\beta}} \gamma_\beta \beta(\mathbf{x}), \quad \mathbf{x} \in \mathbb{N}^2, \quad (38)$$

where  $\mathbf{\beta}$  denotes the set  $\{\beta_{k,l}^{(i,j)}, i, j, k, l \in \mathbb{N}\}$  of functions  $\mathbb{N}^2 \mapsto \{-1, 0, 1\}$  given by

$$\beta_{k,l}^{(i,j)}(i, j) = \beta_{k,l}^{(i,j)}(i+k, j+l) = 1, \quad \beta_{k,l}^{(i,j)}(i+k, j) = \beta_{k,l}^{(i,j)}(i, j+l) = -1,$$

and  $\beta_{k,l}^{(i,j)} = 0$  elsewhere.

Having in mind the identity  $a_j - b_j = \left(\sum_{k=0}^j a_k - \sum_{k=0}^j b_k\right) - \left(\sum_{k=0}^{j-1} a_k - \sum_{k=0}^{j-1} b_k\right)$ , and in the spirit of (38), we see from (32) and (33) the following relation between the pmfs of  $(\check{I}_v, \check{H}_v)$  and  $(\check{I}_w, \check{H}_w)$ :

$$p_{\check{I}_w, \check{H}_w}(\mathbf{x}) = p_{\check{I}_v, \check{H}_v}(\mathbf{x}) + \sum_{j=0}^{\infty} \left( \sum_{k=0}^j a_k - \sum_{k=0}^j b_k \right) \beta_{1,1}^{(0,j)}(\mathbf{x}). \quad (39)$$

The coefficients  $\left(\sum_{k=0}^j a_k - \sum_{k=0}^j b_k\right)$  in (39) are nonnegative for all  $j \in \mathbb{N}$ , from the assumption  $H_v^{\tau_v} \leq_{st} H_w^{\tau_w}$ . The coefficients are indeed differences of their respective cdfs. Theorem 1 of [Meyer and Strulovici, 2015] conveys, as a result of (39), that  $(\check{I}_v, \check{H}_v) \leq_{sm} (\check{I}_w, \check{H}_w)$ . Evoking Lemma 2 (see Appendix C), we deduce  $\left(\sum_{i=1}^{\check{N}} \check{I}_v, \sum_{i=1}^{\check{N}} \check{H}_v\right) \leq_{sm} \left(\sum_{i=1}^{\check{N}} \check{I}_w, \sum_{i=1}^{\check{N}} \check{H}_w\right)$ , with the same assumptions on the involved random variables as in (37). From Corollary 9.A.10 of [Shaked and Shanthikumar, 2007], with  $Y$  independent of the other random variables, it follows that  $\left(\sum_{i=1}^{\check{N}} \check{I}_v, \sum_{i=1}^{\check{N}} \check{H}_v + Y\right) \leq_{sm} \left(\sum_{i=1}^{\check{N}} \check{I}_w, \sum_{i=1}^{\check{N}} \check{H}_w + Y\right)$ . Finally, referring to (37), we conclude  $(N_v, M) \leq_{sm} (N_w, M)$ .  $\square$

## B Proof of Theorem 3

Let  $N^* = (N_i, i \in \mathcal{V}^*)$  and  $M^* = \sum_{i \in \mathcal{V}^*} N_i$ . Given Corollary 1 of [Côté et al., 2024],  $N^* \sim \text{MPMRF}(\lambda, \alpha \mathbf{1}_{|\mathcal{E}^*|}, \tau^*)$ . By Theorem 2, since  $H_v^{\tau_v} \leq_{st} H_w^{\tau_w}$ , we have

$$(N_v, M^*) \leq_{sm} (N_w, M^*). \quad (40)$$

Also,  $(N_w, M^*) \stackrel{d}{=} (N'_w, M^{*'})$  because the only elements of discordance,  $N_u$  and  $N'_u$ , are not part of  $M^*$  nor  $M^{*'}$ . Hence, given relation (40),  $(N_v, M^*) \leq_{sm} (N'_w, M^{*'})$ . By Theorem 9.A.14 of [Shaked and Shanthikumar, 2007], the relation

$$\left( \sum_{i=1}^{N_v} I_i^{(\alpha_{(u,v)})}, M^* \right) \leq_{sm} \left( \sum_{i=1}^{N'_w} I_i^{(\alpha'_{(u,w)})}, M^{*''} \right) \quad (41)$$

also holds. Recall that  $\alpha_{(u,v)} = \alpha'_{(u,w)}$ . Then, by Corollary 9.A.10 of [Shaked and Shanthikumar, 2007], relation in (41) becomes

$$\left( \sum_{i=1}^{N_v} I_i^{(\alpha_{(u,v)})} + L_u, M^* \right) \leq_{sm} \left( \sum_{i=1}^{N'_w} I_i^{(\alpha'_{(u,w)})} + L'_u, M^{*''} \right), \quad (42)$$

since  $L_u \stackrel{d}{=} L'_u$ , and both are independent of all other implicated random variables. Rewriting (42), we have

$$(N_u, M^*) \leq_{sm} (N'_u, M^{*''}). \quad (43)$$

Note that  $\{N_j, j \in \mathcal{V}^\dagger \setminus \{u\}\} \stackrel{d}{=} \{N'_j, j \in \mathcal{V}^\dagger \setminus \{u\}\}$ , since their dependence relations are not affected by the change in the anchorage of vertex  $u$  given the global Markov property. Similarly, for every  $j \in \mathcal{V}^\dagger$ ,

$$(N_j | N_{\text{pa}(j)} = \theta) \stackrel{d}{=} (N'_j | N'_{\text{pa}(j)} = \theta), \quad \theta \in \mathbb{N}, \quad (44)$$

with the filial relation taken according to a root chosen among  $\mathcal{V}^*$ . Besides, because  $(N_j | N_v = \theta)$  follows a binomial distribution of size parameter  $\theta$ , the order relation

$$(N_j | N_{\text{pa}(j)} = \theta_1) \leq_{st} (N_j | N_{\text{pa}(j)} = \theta_2), \quad \theta_1, \theta_2 \in \mathbb{N}, \quad \theta_1 \leq \theta_2 \quad (45)$$

holds for all  $j \in \mathcal{V}^\dagger$ . In the same vein,

$$(N'_j | N'_{\text{pa}(j)} = \theta_1) \leq_{st} (N'_j | N'_{\text{pa}(j)} = \theta_2), \quad \theta_1, \theta_2 \in \mathbb{N}, \quad \theta_1 \leq \theta_2. \quad (46)$$

Given the global Markov properties of  $N$  and  $N'$ , and relations (43), (44), (45) and (46), one may then proceed as in the proof of Theorem 6 in [Côté et al., 2024], repeatedly invoking Theorem 9.A.15 of [Shaked and Shanthikumar, 2007] using  $N_u$  and  $N'_u$  as mixing random for the first iteration,  $(N_u, (N_i : i \in \text{ch}(u)))$  for the second, and so on until all random variables associated to vertices constituting  $\tau^\dagger$  are captured. This operation yields

$$(N_u, M^*, (N_j : j \in \mathcal{V}^\dagger \setminus \{u\})) \leq_{sm} (N'_u, M^{*''}, (N'_j : j \in \mathcal{V}^\dagger \setminus \{u\})).$$

From Theorem 3.1 of [Müller, 1997], we deduce  $(N_u + M^* + \sum_{j \in \mathcal{V}^\dagger \setminus \{u\}} N_j) \leq_{cx} (N'_u + M^{*''} + \sum_{j \in \mathcal{V}^\dagger \setminus \{u\}} N'_j)$ , which is the desired result  $M \leq_{cx} M'$ .  $\square$

## C Lemma 2 and Lemma 3

**Lemma 2.** Consider two vectors of random variables  $(X_1, X_2)$  and  $(X'_1, X'_2)$  such that  $(X_1, X_2) \leq_{sm} (X'_1, X'_2)$ . For a random variable  $W$  taking values in  $\mathbb{N}$ , we observe the relation

$$\left( \sum_{i=1}^W X_{1,i}, \sum_{i=1}^W X_{2,i} \right) \leq_{sm} \left( \sum_{i=1}^W X'_{1,i}, \sum_{i=1}^W X'_{2,i} \right),$$

where  $\{(X_{1,i}, X_{2,i}), i \in \mathbb{N}_1\}$  and  $\{(X'_{1,i}, X'_{2,i}), i \in \mathbb{N}_1\}$  are sequences of independent vectors of random variables identically distributed to  $(X_1, X_2)$  and  $(X'_1, X'_2)$  respectively, and are independent of  $W$ .

*Proof.* Since  $x \mapsto x \mathbb{1}_{\{w \geq k\}}$  is increasing, Corollary 9.A.10 of [Shaked and Shanthikumar, 2007] implies that the relation

$$(X_1 \mathbb{1}_{\{W \geq k\}}, X_2 \mathbb{1}_{\{W \geq k\}}) \leq_{sm} (X'_1 \mathbb{1}_{\{W \geq k\}}, X'_2 \mathbb{1}_{\{W \geq k\}})$$

holds for all  $k \in \mathbb{N}$ . Hence, one has  $(X_{1,i} \mathbb{1}_{\{W \geq i\}}, X_{2,i} \mathbb{1}_{\{W \geq i\}}) \leq_{sm} (X'_{1,i} \mathbb{1}_{\{W \geq i\}}, X'_{2,i} \mathbb{1}_{\{W \geq i\}})$ , for all  $i \in \mathbb{N}^*$ . Then, we sum every vector of the sequence  $\{(X_{1,i} \mathbb{1}_{\{W \geq i\}}, X_{2,i} \mathbb{1}_{\{W \geq i\}}), i \in \mathbb{N}^*\}$ , componentwise, and separately  $\{(X'_{1,i} \mathbb{1}_{\{W \geq i\}}, X'_{2,i} \mathbb{1}_{\{W \geq i\}}), i \in \mathbb{N}_1\}$ , while we repeatedly apply Theorem 9.A.12 of [Shaked and Shanthikumar, 2007] to obtain

$$\left( \sum_{i=1}^{\infty} X_{1,i} \mathbb{1}_{\{W \geq i\}}, \sum_{i=1}^{\infty} X_{2,i} \mathbb{1}_{\{W \geq i\}} \right) \leq_{sm} \left( \sum_{i=1}^{\infty} X'_{1,i} \mathbb{1}_{\{W \geq i\}}, \sum_{i=1}^{\infty} X'_{2,i} \mathbb{1}_{\{W \geq i\}} \right),$$

which rewrites  $(\sum_{i=1}^W X_{1,i}, \sum_{i=1}^W X_{2,i}) \leq_{sm} (\sum_{i=1}^W X'_{1,i}, \sum_{i=1}^W X'_{2,i})$ . □

**Lemma 3.** Let  $X = (X_i, i \in \{1, \dots, d\})$  be a vector of random variables taking on values in  $\mathbb{N}^d$  and  $Y$  be the sum of its components. For  $v, w \in \{1, \dots, d\}$ , if

$$\mathbb{E}[X_v \mathbb{1}_{\{Y \geq k\}}] \geq \mathbb{E}[X_w \mathbb{1}_{\{Y \geq k\}}], \quad \text{for every } k \in \mathbb{N}, \quad (47)$$

then  $C_\kappa^{\text{TVaR}}(X_v; Y) \leq C_\kappa^{\text{TVaR}}(X_w; Y)$  for all  $\kappa \in [0, 1)$ .

*Proof.* Fix  $\kappa \in [0, 1)$ . Let  $q_\kappa = \text{VaR}_\kappa(Y)$  and  $\xi_\kappa = \frac{F_Y(q_\kappa) - \kappa}{p_Y(q_\kappa)}$ . Note that  $\xi_\kappa \in [0, 1]$  for every  $\kappa \in [0, 1)$ . Let  $\Delta_\kappa = C_\kappa^{\text{TVaR}}(X_w, Y) - C_\kappa^{\text{TVaR}}(X_v, Y)$ . We do not know whether  $\mathbb{E}[X_v \mathbb{1}_{\{Y = q_\kappa\}}] \geq \mathbb{E}[X_w \mathbb{1}_{\{Y = q_\kappa\}}]$  or vice versa; thus, we prove  $\Delta_\kappa \geq 0$  under both possibilities. If  $\mathbb{E}[X_v \mathbb{1}_{\{Y = q_\kappa\}}] \geq \mathbb{E}[X_w \mathbb{1}_{\{Y = q_\kappa\}}]$ , we have

$$\begin{aligned} \Delta_\kappa &= \frac{1}{1-\kappa} \left( \mathbb{E}[X_w \mathbb{1}_{\{Y \geq q_{\kappa+1}\}}] - \mathbb{E}[X_v \mathbb{1}_{\{Y \geq q_{\kappa+1}\}}] \right) + \xi_\kappa \left( \mathbb{E}[X_w \mathbb{1}_{\{Y = q_\kappa\}}] - \mathbb{E}[X_v \mathbb{1}_{\{Y = q_\kappa\}}] \right) \\ &\geq \frac{1}{1-\kappa} \left( \mathbb{E}[X_w \mathbb{1}_{\{Y \geq q_{\kappa+1}\}}] - \mathbb{E}[X_v \mathbb{1}_{\{Y \geq q_{\kappa+1}\}}] \right) + 1 \times \left( \mathbb{E}[X_w \mathbb{1}_{\{Y = q_\kappa\}}] - \mathbb{E}[X_v \mathbb{1}_{\{Y = q_\kappa\}}] \right) \\ &= \frac{1}{1-\kappa} \left( \mathbb{E}[X_w \mathbb{1}_{\{Y \geq q_\kappa\}}] - \mathbb{E}[X_v \mathbb{1}_{\{Y \geq q_\kappa\}}] \right), \end{aligned}$$

which is positive given (47). Conversely, if  $\mathbb{E}[X_v \mathbb{1}_{\{Y = q_\kappa\}}] \leq \mathbb{E}[X_w \mathbb{1}_{\{Y = q_\kappa\}}]$ , we have

$$\begin{aligned} \Delta_\kappa &\geq \frac{1}{1-\kappa} \left( \mathbb{E}[X_w \mathbb{1}_{\{Y \geq q_{\kappa+1}\}}] - \mathbb{E}[X_v \mathbb{1}_{\{Y \geq q_{\kappa+1}\}}] \right) + 0 \times \left( \mathbb{E}[X_w \mathbb{1}_{\{Y = q_\kappa\}}] - \mathbb{E}[X_v \mathbb{1}_{\{Y = q_\kappa\}}] \right) \\ &= \frac{1}{1-\kappa} \left( \mathbb{E}[X_w \mathbb{1}_{\{Y \geq q_{\kappa+1}\}}] - \mathbb{E}[X_v \mathbb{1}_{\{Y \geq q_{\kappa+1}\}}] \right), \end{aligned}$$

which is also positive given (47). Therefore, the inequality  $\Delta_\kappa$  holds for all  $\kappa \in [0, 1)$ . □

## D Hasse diagrams for the poset defined in Section 4

Let  $\Omega_{\mathcal{T}}^{(d)}$  be the set of all distinct  $n_d$  trees of  $d$  nodes  $\mathcal{V} = \{1, \dots, d\}$ . Note that  $n_d = 2, 3, 6, 11, 23, 47$  for  $d = 4, 5, 6, 7, 8, 9$  respectively (see Enumeration of trees in [Knuth, 1997], pp 386-388, or sequence A000055 from OEIS for details about the computation of  $n_d$ ). In Appendix 3 of [Harary, 2018], one finds the depictions of all the

elements within the set  $\Omega_T^{(d)}$  for each  $d \in \{4, \dots, 9\}$ . The partial order introduced in Section 4 allows to establish the relations among the  $n_d$  trees within the finite set  $\Omega_T^{(d)}$  for each  $d \in \{4, \dots, 9\}$ . In Figure 12 (page 22), we depict the Hasse diagrams of the posets  $(\Omega_T^{(d)}, \leq_{sha})$  for every  $d \in \{4, \dots, 9\}$ . The implied orientation of the order is upward, *i.e.*, of two linked trees, the uppermost is greater than the other based on  $\leq_{sha}$ . Notably, these Hasse diagrams prove to be useful to illustrate the minimal and maximal elements in the sense of this partial order of  $(\Omega_T^{(d)}, \leq_{sha})$  for each  $d \in \{4, \dots, 9\}$ . Also, for  $d \in \{4, \dots, 8\}$ , we observe that  $(\Omega_T^{(d)}, \leq_{sha})$  is a lattice.

## Acknowledgments

This work was partially supported by the Natural Sciences and Engineering Research Council of Canada (Cossette: 04273; Marceau: 05605; Côté), by the Fonds de recherche du Québec – Nature et technologie (Côté: 335878), and by the Chaire en actuariat de l’Université Laval (Cossette, Côté, Marceau: FO502320).

## References

- Ansari, J. and Rüschendorf, L. (2024). Supermodular and directionally convex comparison results for general factor models. *Journal of Multivariate Analysis*, 201:105264.
- Barghi, A. and DeFord, D. (2024). Ranking trees based on global centrality measures. *Discrete Applied Mathematics*, 343:231–257.
- Besag, J. (1974). Spatial interaction and the statistical analysis of lattice systems. *Journal of the Royal Statistical Society: Series B (Methodological)*, 36(2):192–225.
- Blier-Wong, C., Cossette, H., and Marceau, E. (2022). Generating function method for the efficient computation of expected allocations. *arXiv preprint arXiv:2207.02654*.
- Borgatti, S. P. (2005). Centrality and network flow. *Social Networks*, 27(1):55–71.
- Borgatti, S. P., Agneessens, F., Johnson, J. C., and Everett, M. G. (2024). *Analyzing Social Networks*. SAGE publications Ltd, 2 edition.
- Borgatti, S. P. and Everett, M. G. (2006). A graph-theoretic perspective on centrality. *Social Networks*, 28(4):466–484.
- Borgatti, S. P., Mehra, A., Brass, D. J., and Labianca, G. (2009). Network analysis in the social sciences. *Science*, 323(5916):892–895.
- Bresler, G. and Karzand, M. (2020). Learning a tree-structured Ising model in order to make predictions. *Annals of Statistics*.
- Burt, R. S. (1991). *STRUCTURE Version 4.2 Reference Manual*. Center for the Social Sciences, Columbia University.
- Chow, C. and Liu, C. (1968). Approximating discrete probability distributions with dependence trees. *IEEE transactions on Information Theory*, 14(3):462–467.
- Cressie, N. and Wikle, C. K. (2015). *Statistics for Spatio-Temporal Data*. John Wiley & Sons.
- Csikvári, P. (2010). On a poset of trees. *Combinatorica*, 30(2):125–137.
- Csikvári, P. (2013). On a poset of trees ii. *Journal of Graph Theory*, 74(1):81–103.
- Côté, B., Cossette, H., and Marceau, E. (2024). Tree-structured markov random fields with poisson marginal distributions. *Submitted for publication*.
- Denuit, M. and Dhaene, J. (2012). Convex order and comonotonic conditional mean risk sharing. *Insurance: Mathematics and Economics*, 51(2):265–270.

- Dhaene, J., Tsanakas, A., Valdez, E. A., and Vanduffel, S. (2012). Optimal capital allocation principles. *Journal of Risk and Insurance*, 79(1):1–28.
- Fiedler, M. (1973). Algebraic connectivity of graphs. *Czechoslovak mathematical journal*, 23(2):298–305.
- Freeman, L. C. (1979). Centrality in social networks: Conceptual clarification. *Social Networks*, 1:238–263.
- Friedkin, N. E. (1991). Theoretical foundations for centrality measures. *American Journal of Sociology*, 96(6):1478–1504.
- Gölppek, H. T. (2024). Closeness of some tree structures. *Soft Computing*, 28(7):5751–5763.
- Grone, R. and Merris, R. (1987). Algebraic connectivity of trees. *Czechoslovak Mathematical Journal*, 37(4):660–670.
- Grone, R. and Merris, R. (1990). Ordering trees by algebraic connectivity. *Graphs and Combinatorics*, 6(3):229–237.
- Gutman, I., Deng, H., and Radenkovic, S. (2011). The Estrada index: an updated survey. In Cvetkovic, D. M., editor, *Selected Topics on Applications of Graph Spectra*, pages 155–174. Matematički institut SANU, Belgrade.
- Harary, F. (2018). *Graph Theory*. CRC Press.
- Hue, N. T. K. and Chiogna, M. (2021). Structure learning of undirected graphical models for count data. *Journal of Machine Learning Research*, 22(50):1–53.
- Inouye, D. I., Yang, E., Allen, G. I., and Ravikumar, P. (2017). A review of multivariate distributions for count data derived from the Poisson distribution. *Wiley Interdisciplinary Reviews: Computational Statistics*, 9(3):e1398.
- Kızıldemir, B. and Privault, N. (2017). Supermodular ordering of Poisson and binomial random vectors by tree-based correlations. *Probability and Mathematical Statistics*, 38(2):385–405.
- Knuth, D. E. (1997). *The Art of Computer Programming, volume 1 Fundamental Algorithms*. Addison Wesley Longman Publishing Co., Inc.
- Lauritzen, S. L. (1996). *Graphical Models*. Clarendon Press.
- Li, S. and Yu, Y. (2021). On a poset of trees revisited. *Advances in Applied Mathematics*, 127:102164.
- Liu, M., Liu, B., and You, Z. (2009). The majorization theorem of connected graphs. *Linear algebra and its applications*, 431(5-7):553–557.
- Marshall, A. W., Olkin, I., and Arnold, B. C. (2011). *Inequalities: Theory of Majorization and Its Applications*. Springer Series in Statistics.
- Matúš, F. (1992). On equivalence of Markov properties over undirected graphs. *Journal of Applied Probability*, 29(3):745–749.
- Mausser, H. and Romanko, O. (2018). Long-only equal risk contribution portfolios for CVaR under discrete distributions. *Quantitative Finance*, 18(11):1927–1945.
- McKay, B. D. (1977). On the spectral characterisation of trees. *Ars Combinatoria*, 3:219–232.
- Meyer, M. and Strulovici, B. (2015). Beyond correlation: Measuring interdependence through complementarities. *Discussions Series, Department of Economics, University of Oxford*.
- Müller, A. (1997). Stop-loss order for portfolios of dependent risks. *Insurance: Mathematics and Economics*, 21(3):219–223.
- Müller, A. (2013). Duality theory and transfers for stochastic order relations. *Stochastic Orders in Reliability and Risk: In Honor of Professor Moshe Shaked*, pages 41–57.

- Müller, A. and Stoyan, D. (2002). *Comparison Methods for Stochastic Models and Risks*. Wiley.
- Nguyen, H. T., Walker, C., and Walker, E. A. (2018). *A First Course in Fuzzy Logic*. Chapman and Hall/CRC.
- Nikolakakis, K. E., Kalogerias, D. S., and Sarwate, A. D. (2021). Predictive learning on hidden tree-structured ising models. *The Journal of Machine Learning Research*, 22(1):2713–2794.
- Overbeck, L. (2000). Allocation of economic capital in loan portfolios. In Franke, J., Stahl, G., and Härdle, W., editors, *Measuring Risk in Complex Stochastic Systems. Lecture Notes in Statistics, vol 147*. Springer, New York.
- Rochat, Y. (2009). Closeness centrality extended to unconnected graphs: The harmonic centrality index. Application of Social Network Analysis conference, Zurich, August 26-29.
- Ruhnau, B. (2000). Eigenvector-centrality—a node-centrality? *Social Networks*, 22(4):357–365.
- Sabidussi, G. (1966). The centrality index of a graph. *Psychometrika*, 31(4):581–603.
- Saoub, K. R. (2021). *Graph Theory: An Introduction to Proofs, Algorithms, and Applications*. CRC Press.
- Schoch, D. (2015). *A positional approach for network centrality*. PhD thesis, Universität Konstanz.
- Shaked, M. and Shanthikumar, J. G. (2007). *Stochastic Orders*. Springer.
- Steutel, F. W., Vervaat, W., and Wolfe, S. J. (1983). Integer-valued branching processes with immigration. *Advances in Applied Probability*, 15(4):713–725.
- Tasche, D. (2007). Capital allocation to business units and sub-portfolios: the Euler principle. *arXiv preprint arXiv:0708.2542*.
- Wainwright, M. J., Jaakkola, T. S., and Willsky, A. S. (2003). Tree-based reparameterization framework for analysis of sum-product and related algorithms. *IEEE Transactions on Information Theory*, 49(5):1120–1146.

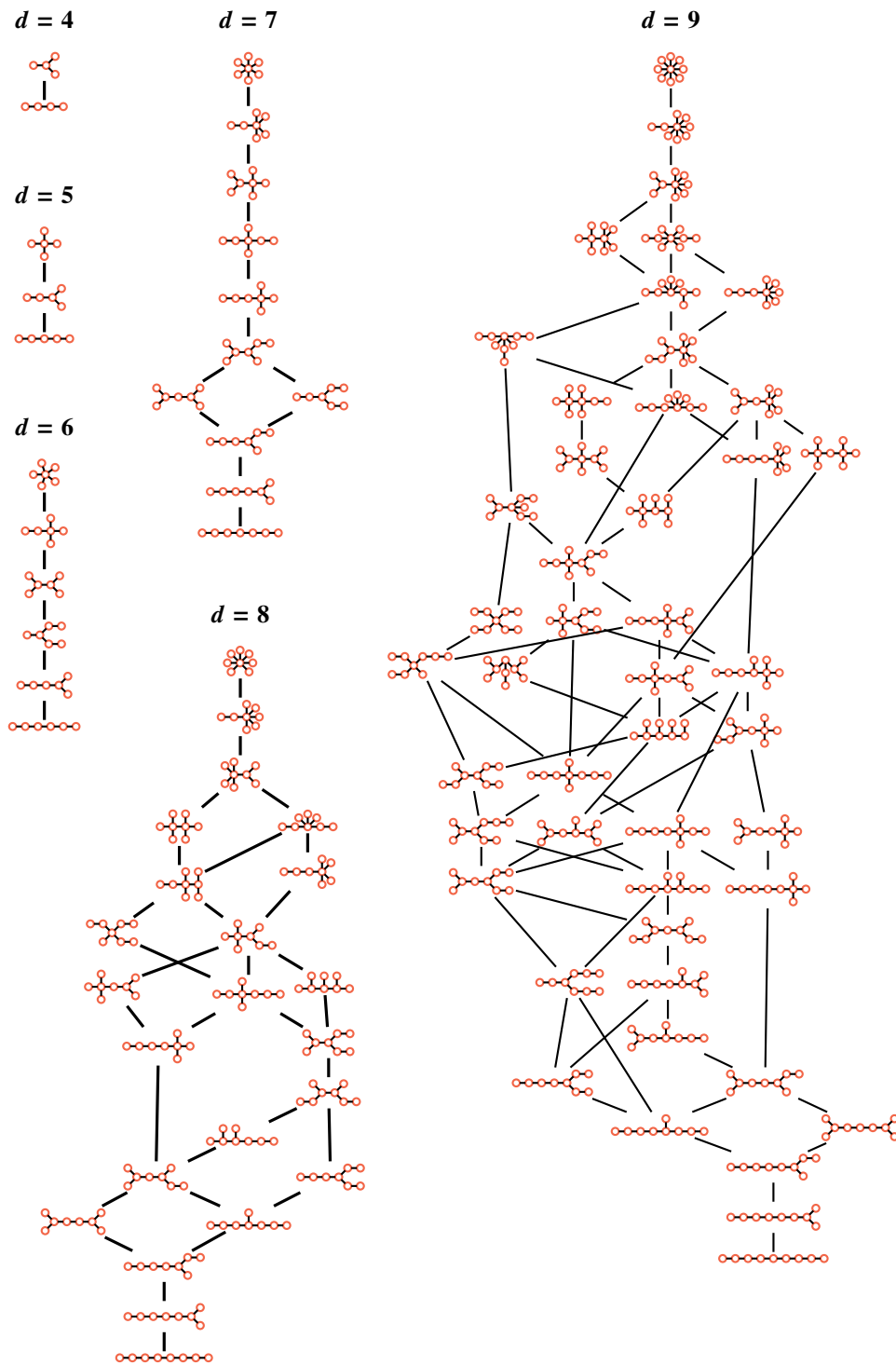


Figure 12: Hasse diagrams of  $(\Omega_{\sigma}^{(d)}, \leq_{sha})$ , for  $d = 4, 5, 6, 7, 8, 9$